

Investigation of Mass and Decay Characteristics of the Light-Strange Tetraquark

Chetan Lodha¹, and Ajay Kumar Rai²,

Department of Physics, Sardar Vallabhbhai National Institute of Technology, Surat, Gujarat-395007, India,
e-mail: iamchetanlodha@gmail.com
e-mail: raiajayk@gmail.com

Received: date / Revised version: date

Abstract. Motivated by recent developments in tetraquark studies, we investigate the mass spectra and decay properties of light-strange tetraquarks ($sq\bar{s}\bar{q}$, $ss\bar{q}\bar{q}$) in diquark-antidiquark formalism. By considering different internal quark structures and internal color structures, mass spectra are generated in semi-relativistic and non-relativistic frameworks. For decay widths, the annihilation model and spectator model have been incorporated. Several resonances have been explored as potential candidates for these tetraquarks. Concurrently, mass spectra and several decay channels of kaons ($s\bar{q}$, $q\bar{s}$) are also investigated. This study is carried out in the hope of helping improve the understanding of tetraquarks in the light-light sector.

1 Introduction

The discovery of the first potential tetraquark candidate in 2003 marks the beginning of a plethora of experimental evidence that compelled physicists worldwide to peer beyond the conventional hadronic structure introduced by Gell-Mann and Zweig in the 1960s [1, 2]. These unconventional or exotic hadrons were theoretically postulated in the 1980s as a result of the success of the quark model [3–6]. Numerous theoretical models have since been employed to probe these exotic hadrons, including Lattice QCD [7], QCD Sum Rule [8], potential models, and phenomenological models [9–12]. These exotic hadrons have been explained by these models as hybrid mesons, tetraquarks, pentaquarks, hadronic molecules, and other structures [13–17].

Four-quark resonances have been interpreted as either compact tetraquarks or meson molecules (also referred to as molecular tetraquarks). Numerous studies have proposed that the possible structures of these multi-quark hadrons can be understood as singlet states [18]. Most tetraquark candidates identified so far include at least one charm quark. Notable discoveries include $Z(4430)$ by Belle [19], $Y(4660)$ by Belle, $Y(4140)$ by Fermilab [20], $X(5568)$ by the $D0$ experiment [21], $Z_c(3900)$ by BESIII [22], and $X(6900)$ by LHCb [23].

In the light-light tetraquark sector, experimental evidence remains scarce. Research on all-strange and all-light tetraquarks is particularly limited, with only a few studies addressing these configurations. Significant theoretical exploration is still required to better understand the properties and structures of all-strange and all-light tetraquarks.

Recent years have seen significant experimental evidence of strange mesons at facilities such as Belle [24], LHCb [25, 26], BaBar [27], and BESIII [28]. Strange mesons and their excitations are abundantly observed in e^+e^- collisions, hadroproduction, and τ -decay. Recent e^+e^- collisions at BaBar and BESIII have provided data for the 2.0–2.2 GeV mass range [29, 30]. Upcoming facilities such as \bar{P} ANDA, LHCb, Belle II, BESIII, and J-PARC aim to improve measurements of strange mesons through in-depth studies of τ -decay [31–38]. J-PARC has also planned the construction of a new kaon beamline. These experimental advancements will enhance our understanding of the unconfirmed strange mesons listed in the PDG. Multiple theoretical models have been developed over the years to explain hadron structures [39–47]. The current study calculates the mass spectra and J^{PC} values for the S, P, D, F, and G waves of kaons.

Compact tetraquarks are often described as bound states of diquarks and anti-diquarks. In the present work, the fitting parameters of mesons are obtained and later employed to derive diquarks and tetraquarks. The mass spectra and decay properties of heavy tetraquarks and heavy-light tetraquarks have been extensively studied in non-relativistic formalism. Semi-relativistic formalism, obtained by incorporating relativistic corrections to kinetic energy, has also successfully determined the mass spectra of heavy-light and heavy-heavy mesons. The heavy tetraquark system has been investigated using the bag model, lattice QCD, QCD sum rules, and potential phenomenological models. Similarly, the mass spectra of other exotic states, such as hadronic molecules, pentaquarks, and hybrid mesons, have been studied in detail in non-relativistic formalism [48].

Correspondence to: iamchetanlodha@gmail.com

Numerous strange closed resonances in the mass range of 1.0–3.5 GeV have been observed in experimental facilities, exhibiting characteristics consistent with four-quark states. Studies suggest that resonances such as η' , $K^*(700)$, $f_0(980)$, $a_0(980)$, $f_0(1370)$, and $f_0(1500)$ are better described as four-quark states than conventional two-quark states.

References [49, 50] propose a tetraquark mixing model that considers light and heavy nonets as tetraquarks formed through the mixing of two tetraquarks. The nature of the $K_0^*(700)$ resonance as a tetraquark candidate has been explored in [51] using $\pi^\pm K_s^0$ correlations. An extensive study of the $qq\bar{q}\bar{q}$ structure is presented in [52], predicting a tetraquark nonet comprising $f_0(600)$, $\kappa(800)$, $f_0(980)$, and $a_0(980)$.

Using QCD Sum Rules, [53] investigates $X(1576)$ as a tetraquark state in the P-wave configuration with scalar diquarks [us], [ds], [$\bar{u}\bar{s}$], and [$\bar{d}\bar{s}$]. Similarly, [54] employs QCD Sum Rules for an in-depth study of fully light vector tetraquark states, explicitly focusing on P-wave configurations, including all-strange and doubly strange light tetraquarks.

References [55, 56] explore the vector resonance $Y(2175)$ as a tetraquark candidate with $s\bar{u}\bar{s}u$ content in a diquark-antidiquark framework using the QCD light-cone sum rule. The present study calculates the mass spectra of S- and P-wave tetraquarks with $sq\bar{s}\bar{q}$ and $ss\bar{q}\bar{q}$ structures. Additionally, the decay properties of these tetraquarks are analyzed, along with their possible decay channels.

The present paper is organized as follows: Section II presents the theoretical framework for determining the mass spectra of mesons, diquarks, and tetraquarks, following a brief introduction in Section I. Section III discusses the mass spectroscopy of diquarks, anti-diquarks, tetraquarks, and kaon mesons. The decay properties of kaons and strange tetraquarks are explored in Section IV. Regge trajectories of kaons and tetraquarks are examined in Section V. The findings and discussion are presented in Section VI, with conclusions provided in Section VII.

2 Theoretical Framework

The current work is motivated by investigations [57–61], where potentials that account for constituent quark interactions for hadrons are inspired by phenomenology. Non-relativistic and semi-relativistic modeling have been used because of the tetraquark's quark composition in the current work. The binding energy of each distinct state is calculated using the modified time-independent radial Schrödinger equation. As described in [62], the center of mass frame is used to incorporate a two-body problem into the central potential model. In order to isolate the radial and angular terms of the time-independent Schrödinger, spherical harmonics have been employed. Using spherical harmonics, the angular and radial terms of the time-independent Schrödinger wave function can be isolated. For mesons and tetraquarks, the fundamental two-body semi-relativistic and non-relativistic Hamiltonian in the center of mass frame, where the motion of constituent particles inside the bound state is relativistic, is given by [63, 64],

$$H_{SR} = \sum_{i=1}^2 \sqrt{p_i^2 + M_i^2} + V^{(0)}(r) + V_{SD}(r), \quad (1)$$

$$H_{NR} = \sum_{i=1}^2 \left(M_i + \frac{p_i^2}{2M_i} \right) + V^{(0)}(r) + V_{SD}(r). \quad (2)$$

where M_i , p_i and $V(r)$ are the constituent mass, relative momentum of the bound state system, and interaction potential, respectively. The kinetic energy term for the non-relativistic Hamiltonian is expanded only up to $\mathcal{O}(p^2)$. On the other hand, the kinetic energy term of the semi-relativistic Hamiltonian is expanded up to $\mathcal{O}(p^{10})$ as

$$\begin{aligned} K.E. = & \sum_{i=1}^2 \frac{p^2}{2} \left(\frac{1}{M_i} \right) - \frac{p^4}{8} \left(\frac{1}{M_i^3} \right) + \frac{p^6}{16} \left(\frac{1}{M_i^5} \right) \\ & - \frac{5p^8}{128} \left(\frac{1}{M_i^7} \right) + \frac{7p^{10}}{256} \left(\frac{1}{M_i^9} \right) \end{aligned} \quad (3)$$

In the expansion up to $\mathcal{O}(p^{10})$, the terms $\mathcal{O}(p^4)$ and $\mathcal{O}(p^8)$ exhibit negative values, while $\mathcal{O}(p^6)$ and $\mathcal{O}(p^{10})$ display positive values. This alternating polarity among the terms suggests a potential cancellation effect, where the positive and negative contributions may partially negate each other. This phenomenon highlights the intricate interplay within the expansion, indicating that certain terms might counterbalance the effects of others, leading to a more refined and accurate description of the system. Notably, the $\mathcal{O}(p^{10})$ term plays a critical role in shaping the mass spectra of light-strange tetraquarks. Its significance becomes evident when considering the delicate balance between the positive and negative contributions, which collectively influence the overall behavior of these particles. The presence of this higher-order term suggests that the expansion's convergence and the resulting mass spectra are particularly sensitive to the inclusion of higher-order contributions. The nuanced dynamics revealed through this balance underscore the importance of carefully considering all relevant terms in the expansion in accurately capturing the mass distribution of strange tetraquarks. The investigation of the hadron spectrum has been studied by various inter-quark interaction potentials [65–67]. Heavy quarkonia spectroscopy has been extensively studied in the zeroth-order Cornell-like potential. This potential comprises a Coulombic potential term and a linear potential term. The Coulombic potential term is a result

of the Lorentz vector exchange employed in the form of one-gluon exchange, whereas the linear potential term arises due to the Lorentz scalar exchange employed in the form of quark confinement. The zeroth-order Cornell-like potential is given by

$$V_{C+L}^{(0)}(r) = \frac{k_s \alpha_s}{r} + br + V_0, \quad (4)$$

where the QCD running coupling constant, color factor, string tension, and constant are given by α_s , k_s , b , and V_0 respectively. The states with color configurations of singlet, triplet-antitriplet, and sextet have color factors of $-\frac{4}{3}$, $-\frac{2}{3}$, and $\frac{1}{3}$, respectively. Inspired by [69], relativistic correction to masses has been incorporated into the central potential. Hence, the central potential has the form,

$$V^{(0)}(r) = V_{C+L}^0(r) + V^1(r) \left(\frac{1}{m_1} + \frac{1}{m_2} \right) \quad (5)$$

where the constituent masses of constituent particles in the bound state are given by m_1 and m_2 . As the non-perturbative form of the relativistic mass correction term is still not studied well enough, the leading order of the perturbation theory is employed [68, 69] and is given as

$$V^1(r) = -\frac{C_F C_A \alpha_s^2}{4 r^2}, \quad (6)$$

where C_F and C_A are the Casimir charges of the fundamental and the adjoint representation with values $\frac{4}{3}$ and 3, respectively.

The incorporation of spin-dependent terms has been done perturbatively for the model, which provides a better understanding of the splitting between the orbital and radial excitations of various states [70].

2.1 Spin-dependent Interactions

The three spin-dependent interactions employed in the present study are inspired by the Breit-Fermi Hamiltonian for one-gluon exchange [70, 71]. By adding the matrix components of interactions as energy corrections using the first-order perturbation theory, the spin-dependent interactions are determined. The tensor V_T interaction potential and spin-orbit interaction potential V_{LS} describe the fine structure of the states, while the hyperfine splitting of the states is described by the spin-spin interaction potential V_{SS} .

$$V_{SD}(r) = V_T(r) + V_{LS}(r) + V_{SS}(r). \quad (7)$$

In terms of the static potential $V(r)$, the spin-interaction potentials are employed. The tensor interaction potential is defined as:

$$V_T = C_T \left(-\frac{1}{3} (S_1 \cdot S_2) + \frac{(S_1 \cdot r)(S_2 \cdot r)}{r^2} \right) \quad (8)$$

where

$$C_T = -\frac{k_s \alpha_s}{4} \frac{12\pi}{M_{\mathcal{Q}} M_{\bar{\mathcal{Q}}}} \frac{1}{r^3} \quad (9)$$

where $M_{\mathcal{Q}}$ and $M_{\bar{\mathcal{Q}}}$ represent the masses of quark and antiquark in the case of mesons. Similarly, in the case of tetraquarks, they represent the masses of diquarks and antidiquarks, respectively. $(S_1 \cdot S_2)$ can be determined by the solution of diagonal matrix elements of spin- $\frac{1}{2}$ and spin-1 particles, as illustrated in ref [72, 73]. Simplifying, the tensor interaction potential equation is as follows:

$$S_{12} = 4 \left[-(S_1 \cdot S_2) + 3(S_1 \cdot r)(S_2 \cdot r) \right] \quad (10)$$

The evaluation of S_{12} is done using Pauli matrices and spherical harmonics with their corresponding eigenvalues. The values of $\langle S_{12} \rangle$ are hence given as [60, 61],

$$\langle S_{12} \rangle_{\frac{1}{2} \otimes \frac{1}{2} \rightarrow S=1, l \neq 0} = \begin{aligned} & -\frac{2l}{2l+3}, \text{ for } J = l+1 \\ & -\frac{2l+2}{2l-1}, \text{ for } J = l-1 \\ & +2, \text{ for } J = l \end{aligned} \quad (11)$$

$\langle S_{12} \rangle$ yields non-zero values for excited states in mesonic states, generalizing $\langle S_{12} \rangle = -4, +2$ and $\frac{2}{3}$, for $J = 0, 1$, and 2 , respectively, but always vanishes for $l = 0$ and $S = 0$. In the case of tetraquarks, spin-1 diquarks are involved, as illustrated in ref [74].

Employing the same formula as used for mesons, the tensor interaction potential of tetraquarks is obtained, except that the wavefunction obtained here will be of spin-1 (anti) diquark [64, 72, 75].

$$\begin{aligned} \langle S_{d-\bar{d}} \rangle &= 12 \left(-\frac{(S_d \cdot S_{\bar{d}})}{3} + \frac{(S_d \cdot r)(S_{\bar{d}} \cdot r)}{r^2} \right) \\ &= S_{14} + S_{13} + S_{24} + S_{23} \end{aligned} \quad (12)$$

where the total spin of the diquark and anti-diquark are given by S_d and $S_{\bar{d}}$, respectively. While obtaining the mass of the tetraquarks by solving the two-body problem, the interaction between the two quarks in the given diquark and the interaction between the two anti-quarks in the anti-diquarks is identical. The spin-orbit interaction potential is defined as [70]:

$$V_{LS} = C_{LS}(L \cdot S) \quad (13)$$

where

$$C_{LS} = -\frac{b}{2M_{\mathcal{Q}}M_{\bar{\mathcal{Q}}}} \frac{1}{r} - \frac{k_s \alpha_s}{2} \frac{3\pi}{M_{\mathcal{Q}}M_{\bar{\mathcal{Q}}}} \frac{1}{r^2} \quad (14)$$

The first term in C_{LS} is known as Thomas precession. This term arises due to the assumption that the confining interaction originates from a Lorentz scalar structure [76, 77]. This term is proportional to the scalar contribution.

By incorporating the spin-spin interactions, a suitable approximation can be obtained for mesons and tetraquarks. A σ parameter has been introduced as a replacement for the Dirac Delta function. The spin-spin interaction potential is defined as [70]:

$$V_{SS} = C_{SS}(S_1 \cdot S_2) \quad (15)$$

where

$$C_{SS} = -\frac{k_s \alpha_s}{3} \frac{8\pi}{M_{\mathcal{Q}}M_{\bar{\mathcal{Q}}}} \frac{\sigma^3}{\sqrt{\pi}} \exp^{-\sigma^2 r^2} \quad (16)$$

For tetraquarks, only the spin-spin interaction is relevant, while the spin-orbit and the tensor interaction are both identically zero considering the fact that the diquarks and anti-diquarks are considered only for the S-wave state. The functional form for spin- $\frac{1}{2}$ particles is based only on the general angular momentum elementary theory [78]. The tensor operator generalized within this approximation can be regarded as the sum of four tensor interactions between four quark-antiquark pairs, which is elucidated in ref [79]. J^{PC} values of different tetraquark states can be obtained by using the relations $P_T = (-1)^{L_T}$ and $C_T = (-1)^{L_T + S_T}$ where S_T and L_T are total spin and total angular momentum, respectively [62]. Coupling S_T and L_T results in total angular momentum J_T , which is used to obtain the mass spectra of radial and orbital excitations. Figure 1b and Figure 1a depict the pictorial representations of the tetraquarks $T_{sq\bar{s}\bar{q}}$ and $T_{ss\bar{q}\bar{q}}$, respectively.

3 Spectroscopy

3.1 Meson Spectra

As inspired by previous studies, the mass spectra of kaons ($q\bar{s}$ and $s\bar{q}$) and pions ($q\bar{q}$) are calculated first, and fitting parameters for diquarks and tetraquarks are obtained from these spectra. The fitting parameters ($M_s, M_q, \alpha_s, b, \sigma$) are calculated in the present work with values $M_s = 0.515 \text{ GeV}$, $M_q = 0.37 \text{ GeV}$, $\alpha_s = 0.9325$, $b = 0.125 \text{ GeV}^2$ and $\sigma = 0.6025 \text{ GeV}$ for kaons ($s\bar{q}$ and $q\bar{s}$). The fitting parameters for pions ($q\bar{q}$) (M_q, α_s, b, σ) in the present work have values $M_q = 0.37 \text{ GeV}$, $\alpha_s = 0.95$, $b = 0.1325 \text{ GeV}^2$ and $\sigma = 0.83 \text{ GeV}$ for pions ($q\bar{q}$). Only colorless quark combinations $|q\bar{q}\rangle$ are permitted to form a color singlet state under SU(3) color symmetry [79]. Kaons ($|q\bar{s}\rangle$ and $|s\bar{q}\rangle$) and pions ($|q\bar{q}\rangle$) exhibit $\bar{\mathbf{3}} \otimes \mathbf{3} = \mathbf{1} \oplus \mathbf{8}$ representation carrying a color factor $k_s = -\frac{4}{3}$ [72]. The masses of each Kaon state ($q\bar{s}$) and ($s\bar{q}$), the Strangeonium state ($s\bar{s}$) and the pion ($q\bar{q}$) states are given by,

$$\begin{aligned} M_{(s\bar{q})} &= M_s + M_{\bar{q}} + E_{(s\bar{q})} + \langle V^1(r) \rangle, \\ M_{(s\bar{s})} &= M_s + M_{\bar{s}} + E_{(s\bar{s})} + \langle V^1(r) \rangle, \\ M_{(q\bar{q})} &= M_q + M_{\bar{q}} + E_{(q\bar{q})} + \langle V^1(r) \rangle. \end{aligned} \quad (17)$$

where $M_s, M_{\bar{s}}, M_q$ and $M_{\bar{q}}$ are constituent masses of strange quark, strange anti-quark, up/down quark, and up/down anti-quark, respectively. Similarly, $E_{(s\bar{q})}, E_{(s\bar{s})}$ and $E_{(q\bar{q})}$ are the binding energies of kaons, strangeonium, and pions, respectively. The final

Table 1: Kaon mass spectra and comparison with PDG [17] and various theoretical models for S, P and D wave in MeV

State	J^{PC}	Meson	Mass _{NR}	Mass _{SR}	[17]	[45]	[67]	[83]	[84]	[85]
1^1S_0	0^-		497	496	497.61 ± 0.013	497.61	462	494	496	482
2^1S_0	0^-		1399	1398		1482.40	1454	1360	1472	1538
3^1S_0	0^-	K(1830)	2011	1966	$1874 \pm 43^{+59}_{-119}$	2036.52	2065	1910	1899	2065
4^1S_0	0^-		2515	2454		2469.27		2210		
1^3S_1	1^-		891	899	891.67 ± 0.26	891.67	903	898	910	897
2^3S_1	1^-		1606	1588		1675.00	1579	1670	1620	1675
3^3S_1	1^-		2161	2094		2194.57	1950	2190		2156
4^3S_1	1^-		2637	2529		2612.79		2490		
1^1P_1	1^+	$K_1(1400)$	1383	1391	1403 ± 7	1286.81	1352	1370	1372	1294
2^1P_1	1^+		1958	1917		1757.00	1897	1980	1841	1757
3^1P_1	1^+		2454	2370		2125.61	2164	2440		2164
4^1P_1	1^+		2896	2808		2439.14				
5^1P_1	1^+									
1^3P_0	0^+		1094	1092		1362.00	1234	1060	1213	1362
2^3P_0	0^+	K(1630)	1686	1645	1630 ± 7	1791.00	1890	1730	1768	1791
3^3P_0	0^+		2188	2103		2135.49	2160	2220		2160
4^3P_0	0^+		2634	2527		2431.66				
1^3P_1	1^+		1418	1438		1403.00	1366	1340	1394	1412
2^3P_1	1^+		1998	1969		1893.00	1928	1960	1850	1893
3^3P_1	1^+		2497	2417		2280.11	2200	2430		2200
4^3P_1	1^+		2939	2835		2610.39				
1^3P_2	2^+	$K_2^*(1430)$	1454	1491	1432.4 ± 1.3	1419.20	1428	1390	1450	1424
2^3P_2	2^+	$K_2^*(1980)$	2045	2028	1994^{+60}_{-50}	1994.00	1938	2020		1896
3^3P_2	2^+		2549	2479		2436.79	2206	2490		2206
4^3P_2	2^+		2996	2900		2810.66				
1^1D_2	2^-	$K_2(1770)$	1742	1727		1750.46	1791	1760	1747	1709
2^1D_2	2^-	$K_2(2250)$	2249	2184	2247 ± 17	2066.00	2238	2290		2066
3^1D_2	2^-		2705	2602		2339.35				
4^1D_2	2^-		3121	3035		2583.95				
1^3D_1	1^-	$K^*(1680)$	1708	1695	1718 ± 18	1700.77	1776	1680	1698	1699
2^3D_1	1^-		2218	2157		2063.00	2251	2210		2063
3^3D_1	1^-		2676	2577		2370.51				
4^3D_1	1^-	$K(3100)$	3094	3004	3100	2642.47				
1^3D_2	2^-		1740	1737		1756.84	1804	1740	1741	1824
2^3D_2	2^-	$K_2(2250)$	2257	2204	2247 ± 17	2163.00	2254	2280		2163
3^3D_2	2^-		2720	2627		2504.13				
4^3D_2	2^-		3142	3057		2804.06				
1^3D_3	3^-		1710	1712		1798.11	1794	1760	1766	1789
2^3D_3	3^-		2236	2210		2182.00	2237	2300		2182
3^3D_3	3^-		2705	2652		2507.80				
4^3D_3	3^-		3130	3052		2795.88				

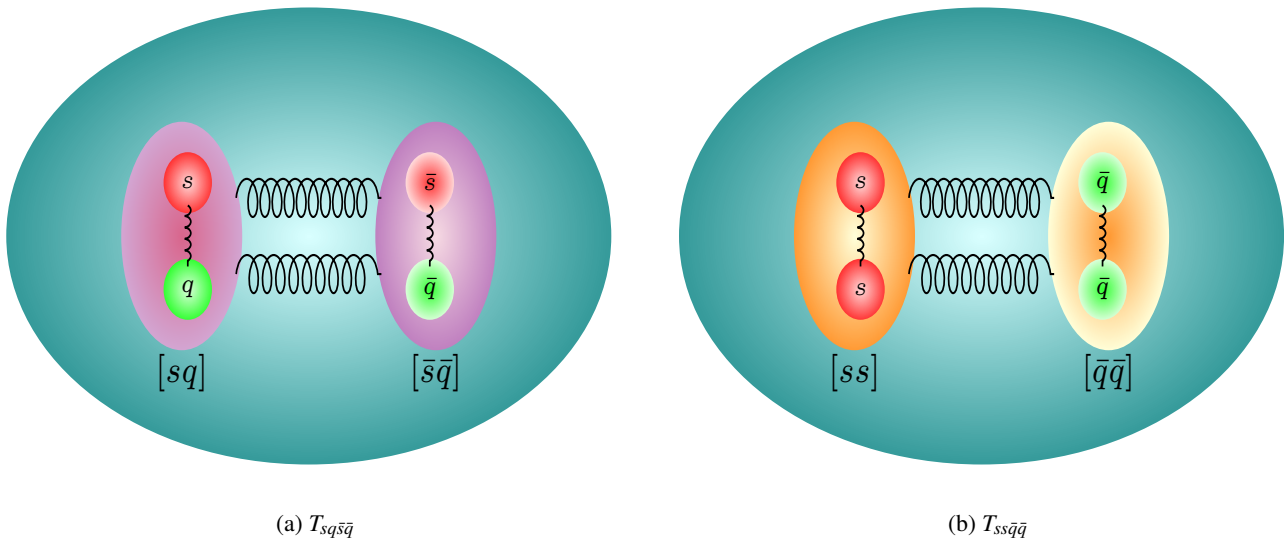


Fig. 1: Pictorial representation of tetraquark $T_{sq\bar{s}\bar{q}}$ and $T_{ss\bar{q}\bar{q}}$

mass derived from the above calculation includes contributions from relativistic mass corrections and spin-dependent terms. A decent agreement is seen between the mass spectra generated in the present study and the experimental data from the most recent updated Particle Data Group [17]. Tables 1 and 2 include the computed mass for kaons as well as comparisons between several theoretical models and PDG.

3.2 Diquarks

A bound state of two quarks or two anti-quarks interacting with each other through gluonic exchange is generally perceived as a diquark (\mathcal{D}) and an anti-diquark ($\bar{\mathcal{D}}$), respectively [80]. Diquarks and anti-diquarks interact, resulting in composite systems rather than point-like objects. As a result of Pauli's exclusion principle, the ground-state wavefunction is of an antisymmetric nature. The diquark's nature can be purely scalar, axial-vector or vector; however, diquarks composed of identical quark flavors can only have spin $S = 1$. Scalar diquarks are dubbed "good diquarks," while axial-vector diquarks are "bad diquarks," which is discussed in [13] in greater detail. The method used to calculate the masses of diquarks and anti-diquarks is the same as for kaons and pions. The fundamental representation for a diquark in QCD color symmetry is represented by $\mathbf{3} \otimes \mathbf{3} = \bar{\mathbf{3}} \oplus \mathbf{6}$ fundamental ($\mathbf{3}$) representation [72]. Likewise, an anti-diquark in the $\bar{\mathbf{3}}$ representation is given by $\bar{\mathbf{3}} \otimes \bar{\mathbf{3}} = \mathbf{3} \oplus \bar{\mathbf{6}}$. A tetraquark is considered a four-body problem since it is composed of two quarks and two anti-quarks. This four-body problem is reduced to a two-body problem by employing the diquark-antidiquark approximation [81]. $\mathbf{1} \otimes \mathbf{1}$ state and the $\mathbf{8} \otimes \mathbf{8}$ state are formed due to the $\bar{\mathbf{3}} \otimes \mathbf{3}$ color coupling. As the color factor k_s in QCD color symmetry for the triplet-antitriplet state is $-\frac{2}{3}$, the short distance part, $\frac{1}{r}$ of the interaction has an attractive nature [79]. The masses of diquarks and anti-diquarks studied in the present work are given by,

$$\begin{aligned}
 M_{(ij)} &= M_i + M_j + E_{(ij)} + \langle V^1(r) \rangle \\
 M_{(\bar{i}\bar{j})} &= M_{\bar{i}} + M_{\bar{j}} + E_{\bar{i}\bar{j}} + \langle V^1(r) \rangle
 \end{aligned}
 \tag{18}$$

where M_i and M_j are masses of constituent quarks in the diquark, while $M_{\bar{i}}$ and $M_{\bar{j}}$ are masses of constituent anti-quarks in the anti-diquark. The mass of all the diquarks calculated in the present work is tabulated in table 3.

3.3 Tetraquark Spectra

A color singlet tetraquark can be materialized by two different diquark-antidiquark combinations: (i) a color anti-triplet diquark and a color triplet anti-diquark, or (ii) a color sextet diquark and a color anti-sextet anti-diquark. Each of these two combinations, held together by color force, forms a tetraquark in a singlet configuration. A tetraquark in the singlet state for $\bar{\mathbf{3}} - \mathbf{3}$ and $\mathbf{6} - \bar{\mathbf{6}}$ has a color factor $k_s = -\frac{4}{3}$ and $-\frac{10}{3}$, respectively [72, 79]. By combining spin-1 diquark and anti-diquark, a singlet tetraquark can

Table 2: Kaon mass spectra and comparison with PDG [17] and various theoretical models for F and G wave in MeV

State	J^P	Meson	Mass _{NR}	Mass _{SR}	[17]	[45]	[67]	[83]	[84]	[85]
1^1F_3	3^+		2043	2010		2114.79	2131	2047		2009
2^1F_3	3^+		2510	2429				2340		
3^1F_3	3^+		2939	2839				2507		
1^3F_2	2^+	$K_2^*(1980)$	2003	1980	1994_{-50}^{+60}	1982.46	2151	2095	1968	1964
2^3F_2	2^+		2476	2404				2364		
3^3F_2	2^+		2910	2818				2519		
1^3F_3	3^+		1994	1980		2050.5	2143	2132		2080
2^3F_3	3^+		2474	2408				2387		
3^3F_3	3^+		2912	2825				2529		
1^3F_4	4^+		1958	2014		2110.04	2108	2080		2096
2^3F_4	4^+		2444	2470				2359		
3^3F_4	4^+		2886	2884				2517		
1^1G_4	4^-		2323	2264		2424.99	2422	2270		2255
2^1G_4	4^-		2759	2663				2476		
1^3G_3	3^-		2259	2214		2228.84	2458	2316		2207
2^3G_3	3^-		2704	2620				2499		
1^3G_4	4^-		2240	2203		2307.08	2433	2337		2285
2^3G_4	4^-		2689	2612				2510		
1^3G_5	5^-	$K_5^*(2380)$	2212	2346	$2382 \pm 19 \pm 14$	2381.46	2388	2291		2356
2^3G_5	5^-		2665	2770				2488		

Table 3: Mass spectra of various diquarks/ anti-diquarks. A comparison with various theoretical models is made. All units are in MeV.

Diquark	Mass _{NR}		Mass _{SR}		[86]	[87]	[88]	[89]	[90]	[91]
	Triplet	Sextet	Triplet	Sextet						
qq	989	1130	942	1126	1020	909	970	840	1060	730
sq	1106	1194	1090	1209	1306	1069	1110	992	1160	
ss	1236	1350	1215	1215	1444	1203	1240	1136	1260	1210

be formed. This singlet tetraquark has the representation $|QQ]^3 \otimes |\bar{Q}\bar{Q}]^3 = \mathbf{1} \oplus \mathbf{8}$. A tetraquark with two strange quarks and two up/down quarks can have more than one internal structure based on the quark flavor of the diquarks or anti-diquarks involved. A $[ss]$ diquark fused with $[qq]$ anti-diquark will result in $T_{ss\bar{q}\bar{q}}$, while a $[sq]$ diquark fused with $[s\bar{q}]$ anti-diquark will result in $T_{sq\bar{s}\bar{q}}$. The $T_{sq\bar{s}\bar{q}}$ tetraquark resembles a quarkonia-like structure, while the $T_{ss\bar{q}\bar{q}}$ resembles a kaonic structure. Hence, the mass spectra for $T_{sq\bar{s}\bar{q}}$ and $T_{ss\bar{q}\bar{q}}$ have the formulation,

$$\begin{aligned}
M_{(SQ\bar{s}\bar{Q})} &= M_{SQ} + M_{\bar{s}\bar{Q}} + E_{(SQ\bar{s}\bar{Q})} + \langle V^1(r) \rangle \\
M_{(SS\bar{Q}\bar{Q})} &= M_{SS} + M_{\bar{Q}\bar{Q}} + E_{(SS\bar{Q}\bar{Q})} + \langle V^1(r) \rangle.
\end{aligned} \tag{19}$$

The Cornell-like potential V_{C+L}^0 , the relativistic term $\langle V^1(r) \rangle$, and the spin-dependent contributions contribute to the mass spectra of the calculated tetraquark states. All the spin-dependent contributions are calculated individually. By coupling total spin S_T with orbital angular momentum L_T , $S_T \otimes L_T$, the color singlet state of the tetraquark is obtained.

$$|T\rangle = |S_d, S_{\bar{d}}, S_T, L_T\rangle_{J_T}, \tag{20}$$

where S_d and $S_{\bar{d}}$ are the spins of diquark and anti-diquark, respectively. In the case of mesons, diquarks, and anti-diquarks, only two spin combinations were possible. However, in the case of a tetraquark, three spin combinations are possible while using spin-1 diquarks and anti-diquarks.

$$\begin{aligned}
|0^{++}\rangle_T &= |S_d = 1, S_{\bar{d}} = 1, S_T = 0, L_T = 0\rangle_{J_T=0}; \\
|1^{+-}\rangle_T &= |S_d = 1, S_{\bar{d}} = 1, S_T = 1, L_T = 0\rangle_{J_T=1}; \\
|2^{++}\rangle_T &= |S_d = 1, S_{\bar{d}} = 1, S_T = 2, L_T = 0\rangle_{J_T=2};
\end{aligned} \tag{21}$$

Utilizing the one-gluon exchange between a quark from a diquark and an anti-quark from an anti-diquark $\mathbf{6} \otimes \bar{\mathbf{6}}$ and $\bar{\mathbf{3}} \otimes \mathbf{3}$ states can be mixed. However, for this mixing to occur, a four-body problem approach for tetraquarks must be considered. Since the current work employs the diquark-antidiquark approximation to treat the tetraquark as a two-body problem, a mixed-state tetraquark cannot be formed. On the other hand, the $\mathbf{6} \otimes \bar{\mathbf{6}}$ configuration is found to be highly suppressed when compared to the $\bar{\mathbf{3}} \otimes \mathbf{3}$ configuration [82]. Due to the repulsive nature of the sextet diquark, the $\bar{\mathbf{3}} \otimes \mathbf{3}$ component in the composite wave function completely dominates the $\mathbf{6} \otimes \bar{\mathbf{6}}$ component. A four-body approach suggests that $\bar{\mathbf{3}} \otimes \mathbf{3}$ and $\mathbf{6} \otimes \bar{\mathbf{6}}$ states behave as two individual states even though they can mix [72]. The mass spectra of $\bar{\mathbf{3}} \otimes \mathbf{3}$ and $\mathbf{6} \otimes \bar{\mathbf{6}}$ states for S wave and P wave for $ss\bar{q}\bar{q}$ and $sq\bar{s}\bar{q}$ are done in tables 4 and 5, respectively. The various two-meson thresholds possible for $ss\bar{q}\bar{q}$ and $sq\bar{s}\bar{q}$ have been tabulated in table 6. The parameter sensitivity of the current theoretical model for mass spectra has been discussed in great detail in our previous work [58].

4 Decay

Decay widths of bound states entail important properties about their internal structures. As a four-body problem, the dynamics of the decay mechanism for tetraquarks are seemingly very complex. The present work studies the decay properties of kaons as well as the tetraquark states. For kaons, various decay channels involving leptonic and radiative decays are studied. For tetraquarks, rearrangement phenomena and strong decay are employed, inspired by ref. [58, 92, 93]. Following that, the diquark-antiannihilation model is employed, which is an extension to quark-annihilation for mesons [63], for gluonic, leptonic, and photonic decay channels. Lastly, the indirect decay of tetraquark by leptonic, photonic, and similar decay channels of the hadrons from the rearrangement model is calculated.

4.1 Annihilation decay

Annihilation decay for tetraquarks treats the diquark and anti-diquarks in a manner similar to the quark-antiquark annihilation for heavy quarkonia. Hence, the same formulation has been extended to the tetraquark model, giving us leptonic, gluonic, and photonic decay. The annihilation decay for T_{3S_1} and T_{1S_0} tetraquark states in $\bar{\mathbf{3}} \otimes \mathbf{3}$ diquark-antidiquark color configuration and T_{1S_0} tetraquark states in $\bar{\mathbf{3}} \otimes \mathbf{3}$ diquark-antidiquark color configuration $\mathbf{6} \otimes \bar{\mathbf{6}}$ has been tabulated in table 7. The total decay rate for a tetraquark with a diquark-antidiquark color configuration $\bar{\mathbf{3}} \otimes \mathbf{3}$ and $\mathbf{6} \otimes \bar{\mathbf{6}}$ are tabulated in table 8.

An essential quantity in the study of hadron decay processes is the square modulus of the wave function at the origin, $|\psi(0)|^2$, which is particularly important for calculating decay widths. In quantum mechanics, the wave function or its derivative at the origin plays a critical role in determining the properties of bound states. Specifically, for quarkonium models, the Schrödinger equation includes a centrifugal term that introduces what is known as a "centrifugal barrier." This barrier limits the calculation of the wave function at the origin to states with orbital angular momentum $l = 0$ (S-states), where the wave function does not vanish. For excited states with $l \neq 0$, the centrifugal barrier causes the wave function at the origin to vanish, making it impossible to calculate $|\psi(0)|^2$ directly for these states. The relationship can be expressed as [70]:

$$|\psi(0)|^2 = |Y_{00}(\theta, \phi)R_{nl}(0)|^2 = \frac{|R_{nl}(0)|^2}{4\pi}$$

Here, $|R_{nl}(0)|^2$ represents the square modulus of the radial wave function at the origin, which can be obtained through numerical calculations.

The 1S_0 $sq\bar{s}\bar{q}$ tetraquark annihilates into 2 gluons, while the 3S_1 $sq\bar{s}\bar{q}$ tetraquark annihilates into 3 gluons. The gluonic decay width, including the first-order radiative correction, is given by [94–98]:

$$\Gamma_{1S_0 \, sq\bar{s}\bar{q} \rightarrow gg} = \frac{2\alpha_s^2 |R_{nl}(0)|^2}{3m_{sq}^2} \left(1 + \frac{4.8\alpha_s}{\pi}\right), \tag{22}$$

$$\Gamma_{3S_1 \, sq\bar{s}\bar{q} \rightarrow ggg} = \frac{10(\pi^2 - 9)\alpha_s^3 |R_{nl}(0)|^2}{81\pi m_{sq}^2}, \tag{23}$$

where $\left(1 + \frac{4.8\alpha_s}{\pi}\right)$ is the QCD correction factors for the digluonic decay channels.

Table 4: Mass spectra of Tetraquarks $T_{ss\bar{q}\bar{q}}$ and $T_{sq\bar{s}\bar{q}}$ with $\bar{3} \otimes 3$ diquark-antidiquark configuration. A comparison with various theoretical models as well as two-meson thresholds is made. All units are in MeV.

State	J^{PC}	Semi-Relativistic Mass		Non-Relativistic Mass	
		$sq\bar{s}\bar{q}$	$ss\bar{q}\bar{q}$	$sq\bar{s}\bar{q}$	$ss\bar{q}\bar{q}$
1^1S_0	0^{++}	1563	1552	1760	1767
2^1S_0	0^{++}	2591	2573	2716	2723
3^1S_0	0^{++}	3065	3049	3205	3211
1^3S_1	1^{+-}	1734	1724	1918	1926
2^3S_1	1^{+-}	2633	2618	2760	2768
3^3S_1	1^{+-}	3093	3078	3232	3241
1^5S_2	2^{++}	2077	2071	2236	2243
2^5S_2	2^{++}	2717	2705	2848	2855
3^5S_2	2^{++}	3147	3135	3288	3297
1^1P_1	1^{--}	2506	2489	2632	2637
2^1P_1	1^{--}	2968	2951	3099	3105
3^1P_1	1^{--}	3333	3319	3481	3489
1^3P_0	0^{-+}	2147	2133	2305	2315
2^3P_0	0^{-+}	2666	2651	2823	2832
3^3P_0	0^{-+}	3055	3041	3226	3234
1^3P_1	1^{-+}	2515	2499	2636	2644
2^3P_1	1^{-+}	2970	2955	3101	3109
3^3P_1	1^{-+}	3332	3318	3481	3489
1^3P_2	2^{-+}	2634	2615	2740	2747
2^3P_2	2^{-+}	3071	3055	3191	3200
3^3P_2	2^{-+}	3426	3412	3566	3574
1^5P_1	1^{--}	2153	2139	2304	2314
2^5P_1	1^{--}	2665	2651	2820	2829
3^5P_1	1^{--}	3048	3035	3219	3228
1^5P_2	2^{--}	2615	2598	2719	2727
2^5P_2	2^{--}	3047	3033	3169	3177
3^5P_2	2^{--}	3398	3385	3540	3548
1^5P_3	3^{--}	2793	2774	2875	2881
2^5P_3	3^{--}	3198	3183	3304	3312
3^5P_3	3^{--}	3538	3525	3667	3675

The 3S_1 state of tetraquark $sq\bar{s}\bar{q}$ can annihilate into lepton pairs with decay width given by [99]:

$$\Gamma_{sq\bar{s}\bar{q} \rightarrow e^+e^-} = \frac{4\pi\alpha^2 e_Q^2 f_{sq\bar{s}\bar{q}}}{3M_{sq\bar{s}\bar{q}}} \times \left(1 + 2\frac{m_e^2}{M_{sq\bar{s}\bar{q}}^2}\right) \sqrt{1 - 4\frac{m_e^2}{M_{sq\bar{s}\bar{q}}^2}} \quad (24)$$

$$\Gamma_{sq\bar{s}\bar{q} \rightarrow \mu^+\mu^-} = \frac{4\pi\alpha^2 e_Q^2 f_{sq\bar{s}\bar{q}}}{3M_{sq\bar{s}\bar{q}}} \times \left(1 + 2\frac{m_\mu^2}{M_{sq\bar{s}\bar{q}}^2}\right) \sqrt{1 - 4\frac{m_\mu^2}{M_{sq\bar{s}\bar{q}}^2}} \quad (25)$$

where α is the fine structure constant, e_Q is the electric charge of the diquark in units of the electron charge, m_e is the mass of the electron, m_μ is the mass of the muon, and $M_{sq\bar{s}\bar{q}}$ is the mass of the $sq\bar{s}\bar{q}$ tetraquark.

$|R_{nl}(0)|^2$ plays a crucial role in the analysis of pseudoscalar and vector states, as it directly impacts the calculation of decay constants. These constants are essential for understanding meson decay properties and predicting their branching ratios. Studies,

Table 5: Mass spectra of Tetraquarks $T_{ss\bar{q}\bar{q}}$ and $T_{sq\bar{s}\bar{q}}$ with $\bar{3} \otimes 3$ diquark-antidiquark configuration in $\mathbf{6-\bar{6}}$. A comparison with various theoretical models as well as two-meson thresholds is made. All units are in MeV.

State	J^{PC}	Semi-Relativistic Mass		Non-Relativistic Mass	
		$sq\bar{s}\bar{q}$	$ss\bar{q}\bar{q}$	$sq\bar{s}\bar{q}$	$ss\bar{q}\bar{q}$
1^1S_0	0^{++}	1234	1299	795	853
2^1S_0	0^{++}	2711	2796	3019	3064
3^1S_0	0^{++}	3762	3754	3971	4019
1^1P_1	1^{--}	2581	2568	2777	2826
2^1P_1	1^{--}	3586	3573	3763	3810
3^1P_1	1^{--}	4290	4283	4499	4546
1^3P_0	0^{-+}	634	628	1040	1107
2^3P_0	0^{-+}	2084	2070	2383	2451
3^3P_0	0^{-+}	2965	2953	3264	3330
1^3P_1	1^{-+}	2550	2537	2752	2803
2^3P_1	1^{-+}	3525	3512	3715	3763
3^3P_1	1^{-+}	4223	4215	4446	4491
1^3P_2	2^{-+}	3229	3213	3345	3390
2^3P_2	2^{-+}	4040	4027	4182	4224
3^3P_2	2^{-+}	4679	4671	4865	4905

Table 6: Two meson threshold for different states of tetraquark $ss\bar{q}\bar{q}$ and $sq\bar{s}\bar{q}$

State	Two-meson Threshold	Threshold Mass (Semi-relativistic)	Threshold Mass (Non-relativistic)
$1S_0$	$K_0^\pm(1S)K_0^\mp(1S)$	995	992
	$\eta_s(1S)\pi(1S)$	882	900
$3S_1$	$K_1^*(1S)K_0^\pm(1S)$	1389	1396
	$\phi(1S)\pi(1S)$	1159	1159
	$\rho(1S)\eta_s(1S)$	1518	1533
$5S_2$	$K_1^*(1S)K_1^*(1S)$	1798	1782
	$\rho(1S)\phi(1S)$	1795	1791
$3P_0$	$K_0(1S)K_0(1P)$	1592	1588
	$\eta_s(1S)a_0(1P)$	1641	1618
	$\pi(1S)f_0(1P)$	1393	1386
$3P_1$	$K_0(1S)K_1(1P)$	1915	1934
	$\eta_s(1S)a_1(1P)$	2055	2059
	$\pi(1S)f_1(1P)$	1593	1597
$3P_2$	$K_0(1S)K_2(1P)$	1952	1987
	$\eta_s(1S)a_2(1P)$	2108	2092
	$\pi(1S)f_2(1P)$	1626	1631
$5P_1$	$K_0(1S)K_1(1P)$	1881	1887
	$\eta_s(1S)b_1(1P)$	2018	2020
	$\pi(1S)h_1(1P)$	1572	1575
$5P_2$	$K_1^*(1S)K_1(1P)$	2310	2338
	$\phi(1S)a_1(1P)$	2332	2317
	$\rho(1S)f_1(1P)$	2229	2229
$5P_3$	$K_1^*(1S)K_2(1P)$	2346	2391
	$\phi(1S)a_2(1P)$	2384	2351
	$\rho(1S)f_2(1P)$	2262	2263

Table 7: Annihilation decay rates for various tetraquark channels in MeV

Internal color configuration	Decay Channel	Semi-relativistic	Non-relativistic
$\bar{3} \otimes 3$	$T_{\bar{3}S_1} \rightarrow e^+e^-$	0.188	0.118
	$T_{\bar{3}S_1} \rightarrow \mu^+\mu^-$	0.188	0.118
	$T_{1S_0} \rightarrow 2\gamma$	0.044	0.045
	$T_{\bar{3}S_1} \rightarrow 3\gamma$	39.517×10^{-6}	40.719×10^{-6}
	$T_{1S_0} \rightarrow 2g$	398.776	328.397
	$T_{\bar{3}S_1} \rightarrow 3g$	8.097	6.303
$6 \otimes \bar{6}$	$T_{1S_0} \rightarrow 2g$	1023.99	811.348
	$T_{1S_0} \rightarrow 2\gamma$	0.116	0.108

Table 8: Total Decay of 1^1S_0 $T_{sq\bar{s}\bar{q}}$ and $T_{ss\bar{q}\bar{q}}$ tetraquark in MeV

Internal color configuration	Semi-relativistic	Non-relativistic
$3 \otimes 3$	407.3	334.9
$6 \otimes \bar{6}$	1024.1	811.5

such as [100], have explored the decay constants of light-heavy mesons using relativistic treatments, which provide a detailed description of systems influenced by relativistic effects.

In this work, we estimate the decay constants for the vector state by evaluating the radial wave function at the origin. This approach offers a simplified yet effective method for analyzing tetraquark decay processes and allows for meaningful comparisons with results from more sophisticated relativistic models. The formula is provided by Van-Royen and Weisskopf [58, 101]:

$$f_{sq\bar{s}\bar{q}}^2 = \frac{3|R_{nIV}(0)|^2}{\pi M_{nIV}} \quad (26)$$

where $|R_{nIV}(0)|^2$ and M_{nIV} are the wave function at the origin and the mass of the vector state, respectively.

Moreover, these decay constants are critical for theoretical predictions and comparisons with experimental data, aiding in the validation or refinement of tetraquark behavior models. By accurately calculating $|\psi(0)|^2$ and decay constants, one can gain valuable insights into the strong interaction, the binding energy, and the dynamics of diquark-antidiquark systems.

The 1^1S_0 $sq\bar{s}\bar{q}$ tetraquark annihilates into two photons, while the 3^1S_1 $sq\bar{s}\bar{q}$ tetraquark annihilates into three photons. The photonic decay width, incorporating first-order radiative corrections, is given by [94, 95]:

$$\Gamma_{sq\bar{s}\bar{q} \rightarrow \gamma\gamma} = \frac{3\alpha^2 e_Q^4 |R_{nl}(0)|^2}{m_{sq}^2}, \quad (27)$$

$$\Gamma_{sq\bar{s}\bar{q} \rightarrow \gamma\gamma\gamma} = \frac{4(\pi^2 - 9)\alpha^3 e_Q^6 |R_{nl}(0)|^2}{3\pi m_{sq}^2}, \quad (28)$$

where m_{sq} is the constituent mass of the diquark and $|R_{nl}(0)|^2$ is the square modulus of the radial wave function at the origin.

4.2 Strong Decay

A tetraquark described using diquark-antidiquark formalism can undergo strong decay through the fall-apart mechanism into the corresponding mesons. The partial decay widths for this process across different channels are given by:

$$\Gamma_{T \rightarrow V_1 V_2} = \mathcal{G}_{TV_1 V_2}^2 \frac{\lambda(T, V_1, V_2)}{8\pi} \left(\frac{m_{V_1}^2 m_{V_2}^2}{m_T^2} + \frac{2\lambda^2(T, V_1, V_2)}{3} \right) \quad (29)$$

$$\Gamma_{T \rightarrow S_1 S_2} = \mathcal{G}_{TS_1 S_2}^2 \frac{\lambda(T, S_1, S_2)}{8\pi} \left(m_{S_1} m_{S_2} + \lambda^2(T, S_1, S_2) \right) \quad (30)$$

$$\lambda(m_1, m_2, m_3) = \frac{\sqrt{m_1^4 + m_2^4 + m_3^4 - 2(m_1^2 m_2^2 + m_2^2 m_3^2 + m_1^2 m_3^2)}}{2m_1} \quad (31)$$

where V_1, V_2, S_1 and S_2 are decaying vector and scalar mesons, while $\mathcal{G}_{TV_1 V_2}$ and $\mathcal{G}_{TS_1 S_2}$ are the coupling constants for the processes $T \rightarrow V_1 V_2$ and $T \rightarrow S_1 S_2$ respectively. While comprehensive experimental data on the decay mechanisms of tetraquarks

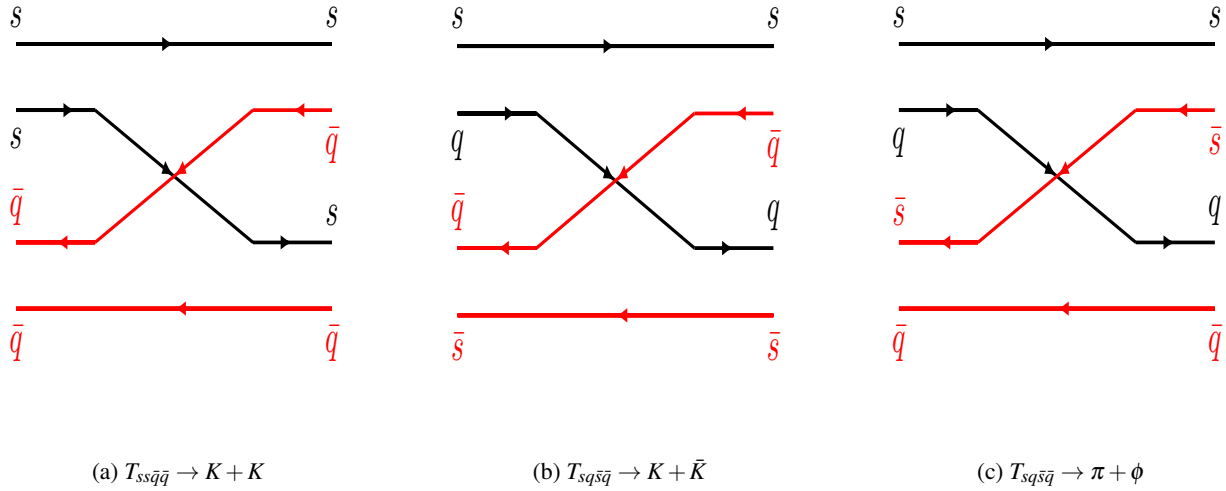


Fig. 2: Rearrangement diagram for Tetraquarks $T_{ss\bar{q}\bar{q}}$ and $T_{sq\bar{s}\bar{q}}$

is still limited, several significant theoretical studies have made important strides in addressing this topic. In our previous work, referenced in [58], we explored the strong decay processes for all-strange tetraquarks. Similarly, the potential decay channels for all-strange tetraquarks were investigated and discussed in reference [102, 103]. Additionally, the authors in references [104–106] employed QCD sum rule methods to assess the strong decay characteristics and coupling constants of all-charm and all-bottom tetraquark states. Moreover, ref. [107] delves into radiative transitions, analyzing the ratios of branching ratios across various decay channels for all-strange tetraquarks, thereby providing valuable theoretical insights into their decay properties. These studies significantly enhance our theoretical understanding of exotic tetraquark systems, shedding light on their decay mechanisms and fundamental properties within the framework of quantum chromodynamics (QCD). The calculated results for various decay channels are summarized in Table 9, offering a comprehensive overview of the current theoretical landscape.

Table 9: Partial decay width for strong decay for various decay channels of all strange tetraquark in semi-relativistic and non-relativistic formalism

Decay Channel	$\lambda_{SR}(GeV)$	$\lambda_{NR}(GeV)$	$\Gamma_{SR}(GeV)$	$\Gamma_{NR}(GeV)$
$T_{ssqq}(0^{++})_{\bar{3}-3} \rightarrow K_0 K_0$	0.5959	0.7311	$0.02273 \mathcal{G}_{T_{ssqq} K_0 K_0}^2$	$0.01425 \mathcal{G}_{T_{ssqq} K_0 K_0}^2$
$T_{ssqq}(2^{++})_{\bar{3}-3} \rightarrow K_1^* K_1^*$	0.5139	0.6811	$0.00671 \mathcal{G}_{T_{ssqq} K_1^* K_1^*}^2$	$0.01177 \mathcal{G}_{T_{ssqq} K_1^* K_1^*}^2$
$T_{ssqq}(0^{++})_{6-\bar{6}} \rightarrow K_0 K_0$	0.4193	-	$0.00703 \mathcal{G}_{T_{ssqq} K_0 K_0}^2$	-
$T_{sqsq}(0^{++})_{\bar{3}-3} \rightarrow K_0 K_0$	0.6031	0.7269	$0.01467 \mathcal{G}_{T_{sqsq} K_0 K_0}^2$	$0.02239 \mathcal{G}_{T_{sqsq} K_0 K_0}^2$
$T_{sqsq}(2^{++})_{\bar{3}-3} \rightarrow K_1^* K_1^*$	0.5199	0.6753	$0.03712 \mathcal{G}_{T_{4s} \eta \eta}^2$	$0.01179 \mathcal{G}_{T_{sqsq} K_1^* K_1^*}^2$
$T_{sqsq}(0^{++})_{6-\bar{6}} \rightarrow K_0 K_0$	0.3670	-	$0.00555 \mathcal{G}_{T_{sqsq} K_0 K_0}^2$	-
$T_{sqsq}(0^{++})_{\bar{3}-3} \rightarrow \pi \eta_s$	0.5937	0.7078	$0.01071 \mathcal{G}_{T_{sqsq} \pi \eta_s}^2$	$0.01708 \mathcal{G}_{T_{sqsq} \pi \eta_s}^2$
$T_{sqsq}(2^{++})_{\bar{3}-3} \rightarrow \phi \rho$	0.6957	0.8010	$0.01120 \mathcal{G}_{T_{sqsq} \phi \rho}^2$	$0.01591 \mathcal{G}_{T_{4s} \phi \rho}^2$
$T_{sqsq}(0^{++})_{6-\bar{6}} \rightarrow \pi \eta_s$	0.3747	-	$0.00359 \mathcal{G}_{T_{sqsq} \pi \eta_s}^2$	-

4.3 Re-arrangement Decay

The recoupling of spin wave functions is given by:

$$\left| \{(ss)^1 (\bar{q}\bar{q})^1 \}^0 \right\rangle = -\frac{1}{2} \left| (s\bar{q})^1 (s\bar{q})^1 \right\rangle^0 + \frac{\sqrt{3}}{2} \left| (s\bar{q})^0 (s\bar{q})^0 \right\rangle^0 \quad (32)$$

$$\begin{aligned} \left| \{ (sq)^1 (\bar{s}\bar{q})^1 \}^0 \right\rangle &= \frac{1}{2} \left(-\frac{1}{2} \left| (s\bar{q})^1 (s\bar{q})^1 \right\rangle^0 + \frac{\sqrt{3}}{2} \left| (s\bar{q})^0 (s\bar{q})^0 \right\rangle^0 \right) \\ &+ \frac{1}{2} \left(-\frac{1}{2} \left| (s\bar{s})^1 (q\bar{q})^1 \right\rangle^0 + \frac{\sqrt{3}}{2} \left| (s\bar{s})^0 (q\bar{q})^0 \right\rangle^0 \right) \end{aligned} \quad (33)$$

Similarly, the recoupling of color wave functions is given by:

$$|(ss)_{\bar{3}}(\bar{q}\bar{q})_{\bar{3}}\rangle = \sqrt{\frac{1}{3}} |(s\bar{q})_{\mathbf{1}}(s\bar{q})_{\mathbf{1}}\rangle - \sqrt{\frac{2}{3}} |(s\bar{q})_{\mathbf{8}}(s\bar{q})_{\mathbf{8}}\rangle \quad (34)$$

$$\begin{aligned} |(sq)_{\bar{3}}(\bar{s}\bar{q})_{\bar{3}}\rangle &= \frac{1}{2} \left(\sqrt{\frac{1}{3}} |(s\bar{s})_{\mathbf{1}}(q\bar{q})_{\mathbf{1}}\rangle - \sqrt{\frac{2}{3}} |(s\bar{s})_{\mathbf{8}}(q\bar{q})_{\mathbf{8}}\rangle \right) + \\ &\frac{1}{2} \left(\sqrt{\frac{1}{3}} |(s\bar{q})_{\mathbf{1}}(s\bar{q})_{\mathbf{1}}\rangle - \sqrt{\frac{2}{3}} |(s\bar{q})_{\mathbf{8}}(s\bar{q})_{\mathbf{8}}\rangle \right) \end{aligned} \quad (35)$$

$$|(ss)_{\mathbf{6}}(\bar{q}\bar{q})_{\bar{\mathbf{6}}}\rangle = \sqrt{\frac{2}{3}} |(s\bar{q})_{\mathbf{1}}(s\bar{q})_{\mathbf{1}}\rangle + \sqrt{\frac{1}{3}} |(s\bar{q})_{\mathbf{8}}(s\bar{q})_{\mathbf{8}}\rangle \quad (36)$$

$$\begin{aligned} |(sq)_{\mathbf{6}}(\bar{s}\bar{q})_{\bar{\mathbf{6}}}\rangle &= \frac{1}{2} \left(\sqrt{\frac{2}{3}} |(s\bar{s})_{\mathbf{1}}(q\bar{q})_{\mathbf{1}}\rangle + \sqrt{\frac{1}{3}} |(s\bar{s})_{\mathbf{8}}(q\bar{q})_{\mathbf{8}}\rangle \right) + \\ &\frac{1}{2} \left(\sqrt{\frac{2}{3}} |(s\bar{q})_{\mathbf{1}}(s\bar{q})_{\mathbf{1}}\rangle + \sqrt{\frac{1}{3}} |(s\bar{q})_{\mathbf{8}}(s\bar{q})_{\mathbf{8}}\rangle \right) \end{aligned} \quad (37)$$

Utilizing the Fierz transformation, various quark-antiquark pairs ($s\bar{s}, s\bar{q}, q\bar{q}$) are brought together [108], and by using the spectator pair method, the tetraquark decays into two mesons. The quark bilinears are normalized to unity. The Fierz re-arrangement for various states employing equations for spin wave function recoupling and color wave function recoupling is given by,

$$\begin{aligned} s\bar{s}\bar{q}q(J=0) &= \left| (ss)_{\bar{3}}^1 (\bar{q}\bar{q})_{\bar{3}}^1 \right\rangle_{\mathbf{1}}^0 \\ &= -\frac{1}{2} \left(\sqrt{\frac{1}{3}} \left| (s\bar{q})_{\mathbf{1}}^1 (s\bar{q})_{\mathbf{1}}^1 \right\rangle_{\mathbf{1}}^0 - \sqrt{\frac{2}{3}} \left| (s\bar{q})_{\mathbf{8}}^1 (s\bar{q})_{\mathbf{8}}^1 \right\rangle_{\mathbf{1}}^0 \right) \\ &+ \frac{\sqrt{3}}{2} \left(\sqrt{\frac{1}{3}} \left| (s\bar{q})_{\mathbf{1}}^0 (s\bar{q})_{\mathbf{1}}^0 \right\rangle_{\mathbf{1}}^0 - \sqrt{\frac{2}{3}} \left| (s\bar{q})_{\mathbf{8}}^0 (s\bar{q})_{\mathbf{8}}^0 \right\rangle_{\mathbf{1}}^0 \right) \end{aligned} \quad (38)$$

$$\begin{aligned} sq\bar{s}\bar{q}(J=0) &= \left| (sq)_{\bar{3}}^1 (\bar{s}\bar{q})_{\bar{3}}^1 \right\rangle_{\mathbf{1}}^0 \\ &= -\frac{1}{4} \left(\sqrt{\frac{1}{3}} \left| (s\bar{q})_{\mathbf{1}}^1 (s\bar{q})_{\mathbf{1}}^1 \right\rangle_{\mathbf{1}}^0 - \sqrt{\frac{2}{3}} \left| (s\bar{q})_{\mathbf{8}}^1 (s\bar{q})_{\mathbf{8}}^1 \right\rangle_{\mathbf{1}}^0 \right) \\ &+ \frac{\sqrt{3}}{4} \left(\sqrt{\frac{1}{3}} \left| (s\bar{q})_{\mathbf{1}}^0 (s\bar{q})_{\mathbf{1}}^0 \right\rangle_{\mathbf{1}}^0 - \sqrt{\frac{2}{3}} \left| (s\bar{q})_{\mathbf{8}}^0 (s\bar{q})_{\mathbf{8}}^0 \right\rangle_{\mathbf{1}}^0 \right) \\ &- \frac{1}{4} \left(\sqrt{\frac{1}{3}} \left| (s\bar{s})_{\mathbf{1}}^1 (q\bar{q})_{\mathbf{1}}^1 \right\rangle_{\mathbf{1}}^0 - \sqrt{\frac{2}{3}} \left| (s\bar{s})_{\mathbf{8}}^1 (q\bar{q})_{\mathbf{8}}^1 \right\rangle_{\mathbf{1}}^0 \right) \\ &+ \frac{\sqrt{3}}{4} \left(\sqrt{\frac{1}{3}} \left| (s\bar{s})_{\mathbf{1}}^0 (q\bar{q})_{\mathbf{1}}^0 \right\rangle_{\mathbf{1}}^0 - \sqrt{\frac{2}{3}} \left| (s\bar{s})_{\mathbf{8}}^0 (q\bar{q})_{\mathbf{8}}^0 \right\rangle_{\mathbf{1}}^0 \right) \end{aligned} \quad (39)$$

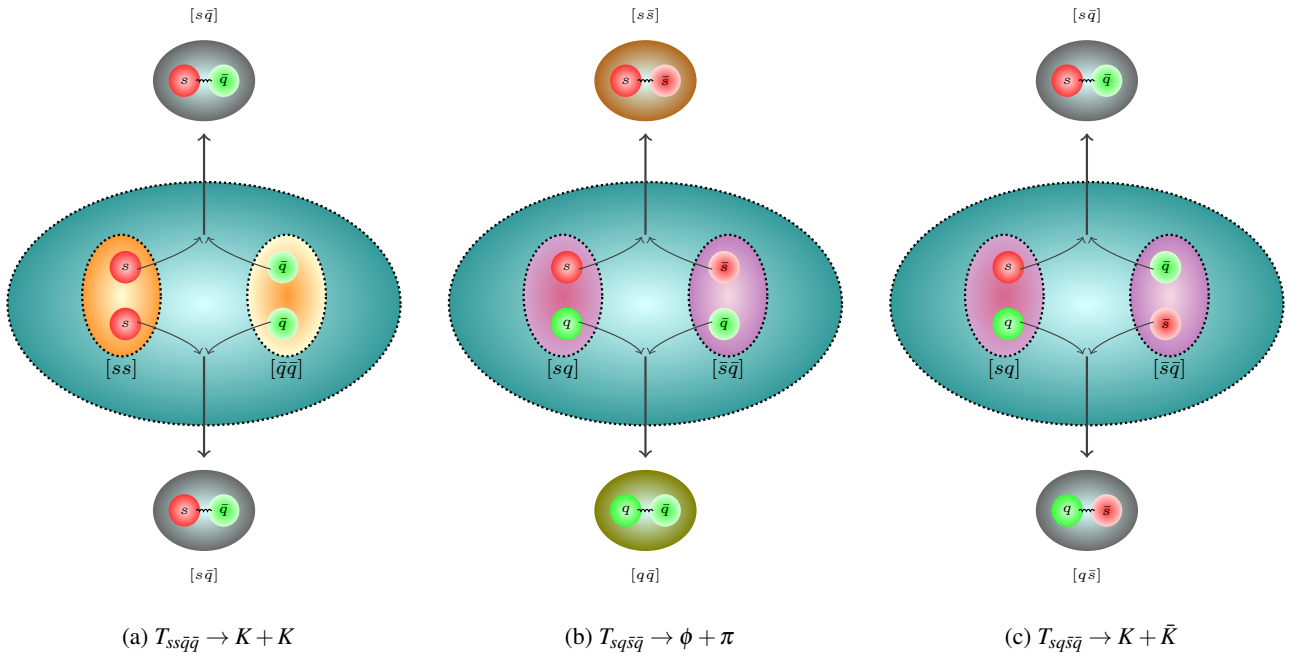


Fig. 3: Pictorial representation of tetraquark re-arrangement

$$\begin{aligned}
 ss\bar{q}\bar{q}(J=0) &= \left| (ss)_6^1 (\bar{q}\bar{q})_6^1 \right\rangle_1^0 \\
 &= -\frac{1}{2} \left(\sqrt{\frac{2}{3}} \left| (s\bar{q})_1^1 (s\bar{q})_1^1 \right\rangle_1^0 + \sqrt{\frac{1}{3}} \left| (s\bar{q})_8^1 (s\bar{q})_8^1 \right\rangle_1^0 \right) \\
 &+ \frac{\sqrt{3}}{2} \left(\sqrt{\frac{2}{3}} \left| (s\bar{q})_1^0 (s\bar{q})_1^0 \right\rangle_1^0 + \sqrt{\frac{1}{3}} \left| (s\bar{q})_8^0 (s\bar{q})_8^0 \right\rangle_1^0 \right)
 \end{aligned} \tag{40}$$

$$\begin{aligned}
 sq\bar{s}\bar{q}(J=0) &= \left| (sq)_6^1 (\bar{s}\bar{q})_6^1 \right\rangle_1^0 \\
 &= -\frac{1}{4} \left(\sqrt{\frac{2}{3}} \left| (s\bar{q})_1^1 (s\bar{q})_1^1 \right\rangle_1^0 + \sqrt{\frac{1}{3}} \left| (s\bar{q})_8^1 (s\bar{q})_8^1 \right\rangle_1^0 \right) \\
 &+ \frac{\sqrt{3}}{4} \left(\sqrt{\frac{2}{3}} \left| (s\bar{q})_1^0 (s\bar{q})_1^0 \right\rangle_1^0 + \sqrt{\frac{1}{3}} \left| (s\bar{q})_8^0 (s\bar{q})_8^0 \right\rangle_1^0 \right) \\
 &- \frac{1}{4} \left(\sqrt{\frac{2}{3}} \left| (s\bar{s})_1^1 (q\bar{q})_1^1 \right\rangle_1^0 + \sqrt{\frac{1}{3}} \left| (s\bar{s})_8^1 (q\bar{q})_8^1 \right\rangle_1^0 \right) \\
 &+ \frac{\sqrt{3}}{4} \left(\sqrt{\frac{2}{3}} \left| (s\bar{s})_1^0 (q\bar{q})_1^0 \right\rangle_1^0 + \sqrt{\frac{1}{3}} \left| (s\bar{s})_8^0 (q\bar{q})_8^0 \right\rangle_1^0 \right)
 \end{aligned} \tag{41}$$

where the color representation's dimensions are denoted using subscripts and the total spin is denoted by a superscript.

The $sq\bar{s}\bar{q}$ tetraquark can be rearranged in two possible manners, namely, $q\bar{s} + s\bar{q}$ and $s\bar{s} + q\bar{q}$ while $ss\bar{q}\bar{q}$ can only rearrange as $q\bar{s} + s\bar{q}$. The decay of various quark-antiquark pairs ($s\bar{s}, s\bar{q}, q\bar{q}$) into lower mass states leads the description of the rearrangement decay. These decays are seen in various channels, which are as follows:

1. The conversion and confinement of two gluons into light hadrons is obtained by the decay of a color singlet spin-0 $s\bar{s}$ pair with a rate of order of α_s^2 . Similarly, the $s\bar{s}$ pair can also convert into 2 photons. With the spectator $q\bar{q}$ pair in account, the decays observed are:

$$\begin{aligned}
 sq\bar{s}\bar{q} &\rightarrow \pi + \text{light hadrons} \\
 sq\bar{s}\bar{q} &\rightarrow \pi + 2\gamma
 \end{aligned}$$

The $q\bar{q}$ pair (π^\pm) can decay into $e^\pm + \nu_e$ and $\mu^\pm + \nu_\mu$ with a rate of order of α^2 . With the spectator $s\bar{s}$ pair in account, the decay observed is:

$$\begin{aligned} sq\bar{s}\bar{q} &\rightarrow \eta_s + e^\pm + \nu_e \\ sq\bar{s}\bar{q} &\rightarrow \eta_s + \mu^\pm + \nu_\mu \end{aligned}$$

2. The conversion and confinement of three gluons into light hadrons are obtained by the decay of color singlet spin-1 pairs with a rate of order of α_s^3 . Successfully, the final states of $\phi + e^+e^-$, $\phi + \mu^+\mu^-$, $\rho + e^+e^-$ and $\rho + \mu^+\mu^-$ are observed with rates of order α_s^2 by annihilating the light hadron into one photon. With the spectator ϕ and π mesons in account, the decays observed are:

$$\begin{aligned} sq\bar{s}\bar{q} &\rightarrow \phi + \text{light hadrons} \\ sq\bar{s}\bar{q} &\rightarrow \rho + \text{light hadrons} \end{aligned}$$

3. The spin-1 $s\bar{s}$ pair in the color octet representation annihilates into one gluon, which materializes into a pair of up or down quarks, which later recombines with the spectator $q\bar{q}$ pair to produce pions, π^\pm , with a rate of order of α_s^2 . The pions further can decay into $\mu^+ + \nu_\mu$ and $e^+ + \nu_e$. The decay observed is:

$$sq\bar{s}\bar{q} \rightarrow \pi + \pi$$

4. The spin-0 $s\bar{s}$ pair in color octet representation annihilates into two gluons, which produce a pair of up or down quarks to neutralize the color of the spectator pair with a rate of order of α_s^2 [109]. The decay observed is:

$$sq\bar{s}\bar{q} \rightarrow \rho + (2g)$$

5. The spin-1 $q\bar{s}$ pair in color singlet representation decays into leptonic channels $e^+ + \nu_e$ and $\mu^+ + \nu_\mu$ when q is up quark. Similarly, the spin-1 $s\bar{q}$ pair decays into leptonic channels $e^- + \nu_e$ and $\mu^- + \nu_\mu$. This conversion occurs with a rate of order of α^2 . With the spectator $q\bar{s}$ and $s\bar{q}$ pairs in account, the decay observed is:

$$\begin{aligned} sq\bar{s}\bar{q}/ss\bar{q}\bar{q} &\rightarrow K^\pm + e^\mp \nu_e \\ sq\bar{s}\bar{q}/ss\bar{q}\bar{q} &\rightarrow K^\pm + \mu^\mp \nu_\mu \end{aligned}$$

6. The spin-1 $q\bar{s}$ pair in color singlet representation can also decay into the rare leptonic channels $\gamma e^+ + \nu_e$ and $\gamma \mu^+ + \nu_\mu$ when q is up quark. Similarly, the spin-1 $s\bar{q}$ pair decays into the rare leptonic channels $\gamma e^- + \nu_e$ and $\gamma \mu^- + \nu_\mu$. This conversion occurs with a rate of order of α^2 . With the spectator $q\bar{s}$ and $s\bar{q}$ pairs in account, the decay observed is:

$$\begin{aligned} sq\bar{s}\bar{q}/ss\bar{q}\bar{q} &\rightarrow K^\pm + \gamma e^\mp \nu_e \\ sq\bar{s}\bar{q}/ss\bar{q}\bar{q} &\rightarrow K^\pm + \gamma \mu^\mp \nu_\mu \end{aligned}$$

The ratio of overlap probabilities of the annihilating $s\bar{s}$ and $q\bar{q}$ pair in $sq\bar{s}\bar{q}$ is proportional to the decay rates:

$$\rho_1 = \frac{|\Psi_{sq\bar{s}\bar{q}}(0)|^2}{|\Psi_\phi(0)|^2} \rho_2 = \frac{|\Psi_{sq\bar{s}\bar{q}}(0)|^2}{|\Psi_\rho(0)|^2} \quad (42)$$

The ratio of overlap probabilities of the decaying $q\bar{s}$ and $s\bar{q}$ pair in $sq\bar{s}\bar{q}/ss\bar{q}\bar{q}$ is proportional to the decay rates:

$$\rho_3 = \frac{|\Psi_{sq\bar{s}\bar{q}}(0)|^2}{|\Psi_{q\bar{s}/s\bar{q}}(0)|^2} \rho_4 = \frac{|\Psi_{ss\bar{q}\bar{q}}(0)|^2}{|\Psi_{q\bar{s}/s\bar{q}}(0)|^2} \quad (43)$$

The individual decay rate is obtained using the simple formula [110]:

$$\Gamma(i)_{color}^{spin} = ||\Psi_{sq\bar{s}\bar{q}/ss\bar{q}\bar{q}}(0)|^2 v \sigma(i)_{color}^{spin} \rightarrow f) \quad (44)$$

where $|\Psi_{sq\bar{s}\bar{q}/ss\bar{q}\bar{q}}(0)|^2$, v , and σ are the overlap probability of the annihilating or decaying pair, relative velocity, and the spin-averaged annihilation/decay cross section in the final state f , respectively. Our previous works [57, 58] and ref. [92, 93] explores the physics of rearrangement decay in further detail. The total of all the individual decay rates yields the total decay rate. The spectator pairs $s\bar{s}$ can appear as η_s or ϕ on the mass shell, or combine with the outgoing $q\bar{q}$ into a pair of open-strange particles for the given tetraquark. Similarly, the spectator pair $q\bar{q}$ can appear as η or π on the mass shell, or combine with the outgoing $s\bar{s}$ into a pair of open-strange particles. Figure 2 depicts the rearrangement diagram for Tetraquarks $T_{sq\bar{s}\bar{q}}$ and $T_{ss\bar{q}\bar{q}}$. Similarly, figure 3 shows a pictorial representation of the rearrangement of Tetraquarks $T_{sq\bar{s}\bar{q}}$ and $T_{ss\bar{q}\bar{q}}$.

A. $\bar{3} - 3$ Tetraquark

The singlet spin 0 decay rate is given by:

$$\begin{aligned}
 \Gamma_1 &= \Gamma(sq\bar{s}\bar{q} \rightarrow \pi + \text{light hadrons}) \\
 &= 2 \cdot \frac{1}{16} \cdot |\Psi_{sq\bar{s}\bar{q}}(0)|^2 v \sigma((s\bar{s}_1^0) \rightarrow 2 \text{ gluons}) \\
 &= \frac{1}{8} \Gamma(\eta_s) \cdot \rho_1 = 0.024 \text{ MeV} \cdot \rho_1
 \end{aligned} \tag{45}$$

$$\begin{aligned}
 \Gamma_2 &= \Gamma(sq\bar{s}\bar{q} \rightarrow \pi + 2\gamma) \\
 &= 2 \cdot \frac{1}{16} \cdot |\Psi_{sq\bar{s}\bar{q}}(0)|^2 v \sigma((s\bar{s}_1^0) \rightarrow 2\gamma) \\
 &= \frac{1}{8} \Gamma(\eta_s \rightarrow 2\gamma) \cdot \rho_1 = 0.094 \text{ keV} \cdot \rho_1
 \end{aligned} \tag{46}$$

$$\begin{aligned}
 \Gamma_3 &= \Gamma(sq\bar{s}\bar{q} \rightarrow \eta_s + e^\pm + \nu_e) \\
 &= 2 \cdot \frac{1}{16} \cdot |\Psi_{sq\bar{s}\bar{q}}(0)|^2 v \sigma((q\bar{q}_1^0) \rightarrow e^\pm + \nu_e) \\
 &= \frac{1}{8} \Gamma(\pi \rightarrow e^\pm + \nu_e) \cdot \rho_2 = 5.906 \text{ eV} \cdot \rho_2
 \end{aligned} \tag{47}$$

$$\begin{aligned}
 \Gamma_4 &= \Gamma(sq\bar{s}\bar{q} \rightarrow \eta_s + \mu^\pm + \nu_\mu) \\
 &= 2 \cdot \frac{1}{16} \cdot |\Psi_{sq\bar{s}\bar{q}}(0)|^2 v \sigma((q\bar{q}_1^0) \rightarrow \mu^\pm + \nu_\mu) \\
 &= \frac{1}{8} \Gamma(\pi \rightarrow \mu^\pm + \nu_\mu) \cdot \rho_2 = 4.797 \text{ MeV} \cdot \rho_2
 \end{aligned} \tag{48}$$

Similarly, the color singlet spin 1 decay rate is given by

$$\begin{aligned}
 \Gamma_5 &= \Gamma(sq\bar{s}\bar{q} \rightarrow \phi + \text{light hadrons}) \\
 &= 2 \cdot \frac{1}{48} \cdot |\Psi_{sq\bar{s}\bar{q}}(0)|^2 v \sigma((q\bar{q}_1^1) \rightarrow 3 \text{ gluons}) \\
 &= \frac{1}{24} \Gamma(\rho) \cdot \rho_2 = 6.142 \text{ MeV} \cdot \rho_2
 \end{aligned} \tag{49}$$

$$\begin{aligned}
 \Gamma_6 &= \Gamma(sq\bar{s}\bar{q} \rightarrow \rho + \text{light hadrons}) \\
 &= 2 \cdot \frac{1}{48} \cdot |\Psi_{sq\bar{s}\bar{q}}(0)|^2 v \sigma((s\bar{s}_1^1) \rightarrow 3 \text{ gluons}) \\
 &= \frac{1}{24} \Gamma(\phi) \cdot \rho_1 = 0.177 \text{ MeV} \cdot \rho_1
 \end{aligned} \tag{50}$$

The annihilation of the spin-1 octet $s\bar{s}$ pair into the light quark pair is given by:

$$\begin{aligned}
 \Gamma_7 &= 2 \cdot \frac{1}{24} \cdot \frac{1}{4} \left(\frac{4\pi\alpha_s^2}{3} \frac{4}{m_\phi^2} \right) |\Psi_\phi(0)|^2 \cdot \rho_1 \\
 &= 0.014 \text{ MeV} \cdot \rho_1
 \end{aligned} \tag{51}$$

The annihilation of the spin-0 octet $s\bar{s}$ pair into the light quark pair is given by:

$$\begin{aligned}
 \Gamma_8 &= 2 \cdot \frac{1}{8} \cdot \frac{1}{4} \left(\frac{4\pi\alpha_s^2}{m_\phi^2} \cdot 18 \right) |\Psi_\phi(0)|^2 \cdot \rho_1 \\
 &= 0.552 \text{ MeV} \cdot \rho_1
 \end{aligned} \tag{52}$$

The leptonic decay of color singlet spin-1 $u\bar{s}$ pair is given by :

$$\begin{aligned}
 \Gamma_9 &= \Gamma(sq\bar{s}\bar{q} \rightarrow K^\pm + e^\mp \nu_e) \\
 &= 2 \cdot \frac{1}{48} \cdot |\Psi_{sq\bar{s}\bar{q}}(0)|^2 v \sigma((K^\pm) \rightarrow e^\mp \nu_e) \\
 &= \frac{1}{24} \frac{G_F^2}{8m_{K^\pm}^3 \pi} f_{K^\pm}^2 [m_e(m_{K^\pm}^2 - m_e^2)]^2 \\
 &= 53.243 \text{ eV} \cdot \rho_3
 \end{aligned} \tag{53}$$

$$\begin{aligned}
 \Gamma_{10} &= \Gamma(sq\bar{s}\bar{q} \rightarrow K^\pm + \mu^\mp \nu_\mu) \\
 &= 2 \cdot \frac{1}{48} \cdot |\Psi_{sq\bar{s}\bar{q}}(0)|^2 v \sigma(K^\pm \rightarrow \mu^\mp \nu_\mu) \\
 &= \frac{1}{24} \frac{G_F^2}{8m_{K^\pm}^3 \pi} f_{K^\pm}^2 [m_\mu(m_{K^\pm}^2 - m_\mu^2)]^2 \\
 &= 2.139 \text{ MeV} \cdot \rho_3
 \end{aligned} \tag{54}$$

$$\begin{aligned}
 \Gamma_{11} &= \Gamma(ss\bar{q}\bar{q} \rightarrow K^\pm + e^\mp \nu_e) \\
 &= 2 \cdot \frac{1}{12} \cdot |\Psi_{ss\bar{q}\bar{q}}(0)|^2 v \sigma((K^\pm) \rightarrow e^\mp \nu_e) \\
 &= \frac{1}{6} \frac{G_F^2}{8m_{K^\pm}^3 \pi} f_{K^\pm}^2 [m_e(m_{K^\pm}^2 - m_e^2)]^2 \\
 &= 212.972 \text{ eV} \cdot \rho_4
 \end{aligned} \tag{55}$$

$$\begin{aligned}
 \Gamma_{12} &= \Gamma(ss\bar{q}\bar{q} \rightarrow K^\pm + \mu^\mp \nu_\mu) \\
 &= 2 \cdot \frac{1}{12} \cdot |\Psi_{ss\bar{q}\bar{q}}(0)|^2 v \sigma(K^\pm \rightarrow \mu^\mp \nu_\mu) \\
 &= \frac{1}{6} \frac{G_F^2}{8m_{K^\pm}^3 \pi} f_{K^\pm}^2 [m_\mu(m_{K^\pm}^2 - m_\mu^2)]^2 \\
 &= 8.556 \text{ MeV} \cdot \rho_4
 \end{aligned} \tag{56}$$

The rare leptonic decay of color singlet spin-1 $u\bar{s}$ pair is given by :

$$\begin{aligned}
 \Gamma_{13} &= \Gamma(sq\bar{s}\bar{q} \rightarrow K^\pm + \gamma e^\mp \nu_e) \\
 &= 2 \cdot \frac{1}{48} \cdot |\Psi_{sq\bar{s}\bar{q}}(0)|^2 v \sigma((K^\pm) \rightarrow \gamma e^\mp \nu_e) \\
 &= \frac{1}{24} \frac{\alpha G_F^2}{2592\pi^2} |V_{su}|^2 f_{K^\pm}^2 m_{K^\pm}^3 (x_u + x_s) \\
 &= 6.395 \text{ eV} \cdot \rho_3
 \end{aligned} \tag{57}$$

$$\begin{aligned}
 \Gamma_{14} &= \Gamma(sq\bar{s}\bar{q} \rightarrow K^\pm + \gamma \mu^\mp \nu_\mu) \\
 &= 2 \cdot \frac{1}{48} \cdot |\Psi_{sq\bar{s}\bar{q}}(0)|^2 v \sigma(K^\pm \rightarrow \gamma \mu^\mp \nu_\mu) \\
 &= \frac{1}{24} \frac{\alpha G_F^2}{2592\pi^2} |V_{su}|^2 f_{K^\pm}^2 m_{K^\pm}^3 (x_u + x_s) \\
 &= 2.165 \text{ keV} \cdot \rho_3
 \end{aligned} \tag{58}$$

$$\begin{aligned}
\Gamma_{15} &= \Gamma(ss\bar{q}\bar{q} \rightarrow K^\pm + \gamma e^\mp \nu_e) \\
&= 2 \cdot \frac{1}{12} \cdot |\Psi_{ss\bar{q}\bar{q}}(0)|^2 v \sigma((K^\pm) \rightarrow \gamma e^\mp \nu_e) \\
&= \frac{1}{6} \frac{\alpha G_F^2}{2592 \pi^2} |V_{su}|^2 f_{K^\pm}^2 m_{K^\pm}^3 (x_u + x_s) \\
&= 25.578 \text{ eV} \cdot \rho_4
\end{aligned} \tag{59}$$

$$\begin{aligned}
\Gamma_{16} &= \Gamma(ss\bar{q}\bar{q} \rightarrow K^\pm + \gamma \mu^\mp \nu_\mu) \\
&= 2 \cdot \frac{1}{12} \cdot |\Psi_{ss\bar{q}\bar{q}}(0)|^2 v \sigma(K^\pm \rightarrow \gamma \mu^\mp \nu_\mu) \\
&= \frac{1}{6} \frac{\alpha G_F^2}{2592 \pi^2} |V_{su}|^2 f_{K^\pm}^2 m_{K^\pm}^3 (x_u + x_s) \\
&= 8.660 \text{ keV} \cdot \rho_4
\end{aligned} \tag{60}$$

where ,

$$x_u = \left(3 - \frac{M_{K^\pm}}{m_u}\right)^2, \quad x_s = \left(3 - 2\frac{M_{K^\pm}}{m_s}\right)^2. \tag{61}$$

where G_F is the Fermi constant, m_u is the mass of the up quark, M_{K^\pm} is the mass of kaon, f_{K^\pm} is the weak decay constant, and $|V_{su}|$ is the element of the CKM matrix, respectively. The branching ratio of various decay channels of $T_{sq\bar{s}\bar{q}}$ and $T_{ss\bar{q}\bar{q}}$ tetraquark in antitriplet-triplet configuration have been tabulated in table 10.

B. 6 – $\bar{6}$ Tetraquark

The singlet spin 0 decay rate is given by:

$$\begin{aligned}
\Gamma_{17} &= \Gamma(sq\bar{s}\bar{q} \rightarrow \pi + \text{light hadrons}) \\
&= 2 \cdot \frac{1}{8} \cdot |\Psi_{sq\bar{s}\bar{q}}(0)|^2 v \sigma((s\bar{s}_1^0) \rightarrow 2 \text{ gluons}) \\
&= \frac{1}{4} \Gamma(\eta_s) \cdot \rho_1 = 0.047 \text{ MeV} \cdot \rho_1
\end{aligned} \tag{62}$$

$$\begin{aligned}
\Gamma_{18} &= \Gamma(sq\bar{s}\bar{q} \rightarrow \pi + 2\gamma) \\
&= 2 \cdot \frac{1}{8} \cdot |\Psi_{sq\bar{s}\bar{q}}(0)|^2 v \sigma((s\bar{s}_1^0) \rightarrow 2\gamma) \\
&= \frac{1}{4} \Gamma(\eta_s \rightarrow 2\gamma) \cdot \rho_1 = 0.188 \text{ keV} \cdot \rho_1
\end{aligned} \tag{63}$$

$$\begin{aligned}
\Gamma_{19} &= \Gamma(sq\bar{s}\bar{q} \rightarrow \eta_s + e^\pm + \nu_e) \\
&= 2 \cdot \frac{1}{8} \cdot |\Psi_{sq\bar{s}\bar{q}}(0)|^2 v \sigma((q\bar{q}_1^0) \rightarrow e^\pm + \nu_e) \\
&= \frac{1}{4} \Gamma(\pi \rightarrow e^\pm + \nu_e) \cdot \rho_2 = 11.812 \text{ eV} \cdot \rho_2
\end{aligned} \tag{64}$$

$$\begin{aligned}
\Gamma_{20} &= \Gamma(sq\bar{s}\bar{q} \rightarrow \eta_s + \mu^\pm + \nu_\mu) \\
&= 2 \cdot \frac{1}{8} \cdot |\Psi_{sq\bar{s}\bar{q}}(0)|^2 v \sigma((q\bar{q}_1^0) \rightarrow \mu^\pm + \nu_\mu) \\
&= \frac{1}{4} \Gamma(\pi \rightarrow \mu^\pm + \nu_\mu) \cdot \rho_2 = 9.594 \text{ MeV} \cdot \rho_2
\end{aligned} \tag{65}$$

Similarly, the color singlet spin 1 decay rate is given by

$$\begin{aligned}
\Gamma_{21} &= \Gamma(sq\bar{s}\bar{q} \rightarrow \phi + \text{light hadrons}) \\
&= 2 \cdot \frac{1}{24} \cdot |\Psi_{sq\bar{s}\bar{q}}(0)|^2 v \sigma((q\bar{q}_1^1) \rightarrow 3 \text{ gluons}) \\
&= \frac{1}{12} \Gamma(\rho) \cdot \rho_2 = 6.142 \text{ MeV} \cdot \rho_2
\end{aligned} \tag{66}$$

$$\begin{aligned}
\Gamma_{22} &= \Gamma(sq\bar{s}\bar{q} \rightarrow \rho + \text{light hadrons}) \\
&= 2 \cdot \frac{1}{24} \cdot |\Psi_{sq\bar{s}\bar{q}}(0)|^2 v \sigma((s\bar{s}_1^1) \rightarrow 3 \text{ gluons}) \\
&= \frac{1}{12} \Gamma(\phi) \cdot \rho_1 = 0.355 \text{ MeV} \cdot \rho_1
\end{aligned} \tag{67}$$

The annihilation of the spin-1 octet $s\bar{s}$ pair into the light quark pair is given by:

$$\begin{aligned}
\Gamma_{23} &= 2 \cdot \frac{1}{48} \cdot \frac{1}{4} \left(\frac{4\pi\alpha_s^2}{3} \frac{4}{m_\phi^2} \right) |\Psi_\phi(0)|^2 \cdot \rho_1 \\
&= 0.007 \text{ MeV} \cdot \rho_1
\end{aligned} \tag{68}$$

The annihilation of the spin-0 octet $s\bar{s}$ pair into the light quark pair is given by:

$$\begin{aligned}
\Gamma_{24} &= 2 \cdot \frac{1}{16} \cdot \frac{1}{4} \left(\frac{4\pi\alpha_s^2}{m_\phi^2} \cdot 18 \right) |\Psi_\phi(0)|^2 \cdot \rho_1 \\
&= 0.276 \text{ MeV} \cdot \rho_1
\end{aligned} \tag{69}$$

The leptonic decay of color singlet spin-1 $u\bar{s}$ pair is given by :

$$\begin{aligned}
\Gamma_{25} &= \Gamma(sq\bar{s}\bar{q} \rightarrow K^\pm + e^\mp \nu_e) \\
&= 2 \cdot \frac{1}{24} \cdot |\Psi_{sq\bar{s}\bar{q}}(0)|^2 v \sigma((K^\pm) \rightarrow e^\mp \nu_e) \\
&= \frac{1}{12} \frac{G_F^2}{8m_{K^\pm}^3 \pi} f_{K^\pm}^2 [m_e(m_{K^\pm}^2 - m_e^2)]^2 \\
&= 106.486 \text{ eV} \cdot \rho_3
\end{aligned} \tag{70}$$

$$\begin{aligned}
\Gamma_{26} &= \Gamma(sq\bar{s}\bar{q} \rightarrow K^\pm + \mu^\mp \nu_\mu) \\
&= 2 \cdot \frac{1}{24} \cdot |\Psi_{sq\bar{s}\bar{q}}(0)|^2 v \sigma((K^\pm) \rightarrow \mu^\mp \nu_\mu) \\
&= \frac{1}{12} \frac{G_F^2}{8m_{K^\pm}^3 \pi} f_{K^\pm}^2 [m_\mu(m_{K^\pm}^2 - m_\mu^2)]^2 \\
&= 4.276 \text{ MeV} \cdot \rho_3
\end{aligned} \tag{71}$$

$$\begin{aligned}
\Gamma_{27} &= \Gamma(ss\bar{q}\bar{q} \rightarrow K^\pm + e^\mp \nu_e) \\
&= 2 \cdot \frac{1}{4} \cdot |\Psi_{ss\bar{q}\bar{q}}(0)|^2 v \sigma((K^\pm) \rightarrow e^\mp \nu_e) \\
&= \frac{1}{2} \frac{G_F^2}{8m_{K^\pm}^3 \pi} f_{K^\pm}^2 [m_e(m_{K^\pm}^2 - m_e^2)]^2 \\
&= 638.916 \text{ eV} \cdot \rho_4
\end{aligned} \tag{72}$$

$$\begin{aligned}
\Gamma_{28} &= \Gamma(ss\bar{q}\bar{q} \rightarrow K^\pm + \mu^\mp \nu_\mu) \\
&= 2 \cdot \frac{1}{4} \cdot |\Psi_{ss\bar{q}\bar{q}}(0)|^2 v \sigma(K^\pm \rightarrow \mu^\mp \nu_\mu) \\
&= \frac{1}{2} \frac{G_F^2}{8m_{K^\pm}^3 \pi} f_{K^\pm}^2 [m_\mu (m_{K^\pm}^2 - m_\mu^2)]^2 \\
&= 25.668 \text{ MeV} \cdot \rho_4
\end{aligned} \tag{73}$$

The rare leptonic decay of color singlet spin-1 $u\bar{s}$ pair is given by :

$$\begin{aligned}
\Gamma_{29} &= \Gamma(sq\bar{s}\bar{q} \rightarrow K^\pm + \gamma e^\mp \nu_e) \\
&= 2 \cdot \frac{1}{24} \cdot |\Psi_{sq\bar{s}\bar{q}}(0)|^2 v \sigma(K^\pm \rightarrow \gamma e^\mp \nu_e) \\
&= \frac{1}{12} \frac{\alpha G_F^2}{2592\pi^2} |V_{su}|^2 f_{K^\pm}^2 m_{K^\pm}^3 (x_u + x_s) \\
&= 12.791 \text{ eV} \cdot \rho_3
\end{aligned} \tag{74}$$

$$\begin{aligned}
\Gamma_{30} &= \Gamma(sq\bar{s}\bar{q} \rightarrow K^\pm + \gamma \mu^\mp \nu_\mu) \\
&= 2 \cdot \frac{1}{24} \cdot |\Psi_{sq\bar{s}\bar{q}}(0)|^2 v \sigma(K^\pm \rightarrow \gamma \mu^\mp \nu_\mu) \\
&= \frac{1}{12} \frac{\alpha G_F^2}{2592\pi^2} |V_{su}|^2 f_{K^\pm}^2 m_{K^\pm}^3 (x_u + x_s) \\
&= 4.331 \text{ keV} \cdot \rho_3
\end{aligned} \tag{75}$$

$$\begin{aligned}
\Gamma_{31} &= \Gamma(ss\bar{q}\bar{q} \rightarrow K^\pm + \gamma e^\mp \nu_e) \\
&= 2 \cdot \frac{1}{4} \cdot |\Psi_{ss\bar{q}\bar{q}}(0)|^2 v \sigma(K^\pm \rightarrow \gamma e^\mp \nu_e) \\
&= \frac{1}{2} \frac{\alpha G_F^2}{2592\pi^2} |V_{su}|^2 f_{K^\pm}^2 m_{K^\pm}^3 (x_u + x_s) \\
&= 76.734 \text{ eV} \cdot \rho_4
\end{aligned} \tag{76}$$

$$\begin{aligned}
\Gamma_{32} &= \Gamma(ss\bar{q}\bar{q} \rightarrow K^\pm + \gamma \mu^\mp \nu_\mu) \\
&= 2 \cdot \frac{1}{12} \cdot |\Psi_{ss\bar{q}\bar{q}}(0)|^2 v \sigma(K^\pm \rightarrow \gamma \mu^\mp \nu_\mu) \\
&= \frac{1}{6} \frac{\alpha G_F^2}{2592\pi^2} |V_{su}|^2 f_{K^\pm}^2 m_{K^\pm}^3 (x_u + x_s) \\
&= 25.98 \text{ keV} \cdot \rho_4
\end{aligned} \tag{77}$$

where ,

$$x_u = \left(3 - \frac{M_{K^\pm}}{m_u}\right)^2, \quad x_s = \left(3 - 2\frac{M_{K^\pm}}{m_s}\right)^2. \tag{78}$$

The branching ratio of various decay channels of $T_{sq\bar{s}\bar{q}}$ and $T_{ss\bar{q}\bar{q}}$ tetraquark in sextet-antisextet configuration have been tabulated in table 10.

5 Regge trajectories

This section discusses regge trajectories of the calculated mass spectrum of Kaon mesons and all strange tetraquarks. Regge trajectories describe the relationship between a particle's spin (or angular momentum, J) and its mass squared (M^2). These trajectories indicate that particles can be grouped into families, each following a nearly linear path in a J versus M^2 plot. For light

Table 10: Branching ratio for various decay channels in spectator model for T_{1S_0}

State	$\mathbf{3-3}$		$\mathbf{6-6}$	
	Semi-Relativistic	Non-Relativistic	Semi-Relativistic	Non-Relativistic
$sq\bar{s}\bar{q} \rightarrow \pi + \text{light hadrons}$	3.569×10^{-4}	2.38258×10^{-4}	8.98094×10^{-4}	8.84389×10^{-4}
$sq\bar{s}\bar{q} \rightarrow \pi + 2\gamma$	1.398×10^{-6}	0.932699×10^{-6}	3.59237×10^{-6}	3.5375×10^{-6}
$sq\bar{s}\bar{q} \rightarrow \eta_s + e^\pm + \nu_e$	8.784×10^{-8}	5.86186×10^{-8}	2.933×10^{-7}	4.624×10^{-7}
$sq\bar{s}\bar{q} \rightarrow \eta_s + \mu^\pm + \nu_\mu$	0.07134	0.04772	0.238232	0.37709
$sq\bar{s}\bar{q} \rightarrow \phi + \text{light hadrons}$	0.09270	0.080579	0.1525	0.2414
$sq\bar{s}\bar{q} \rightarrow \rho + \text{light hadrons}$	0.1187	0.103181	6.783×10^{-3}	6.6799×10^{-3}
$sq\bar{s}\bar{q} \rightarrow \pi + \pi$	2.0823×10^{-4}	1.38918×10^{-4}	1.3375×10^{-4}	1.3178×10^{-4}
$sq\bar{s}\bar{q} \rightarrow \rho + 2g$	8.210×10^{-3}	5.47858×10^{-3}	5.2739×10^{-4}	5.1934×10^{-4}
$sq\bar{s}\bar{q} \rightarrow K^\pm + e^\mp \nu_e$	7.9073×10^{-7}	7.90259×10^{-7}	2.0318×10^{-6}	2.9966×10^{-6}
$sq\bar{s}\bar{q} \rightarrow K^\pm + \mu^\mp \nu_\mu$	0.031767	0.031748	0.081589	0.12033
$ss\bar{q}\bar{q} \rightarrow K^\pm + e^\mp \nu_e$	2.996×10^{-6}	3.34439×10^{-6}	1.142×10^{-5}	1.854×10^{-5}
$ss\bar{q}\bar{q} \rightarrow K^\pm + \mu^\mp \nu_\mu$	0.12037	0.13436	0.4509	0.7449
$sq\bar{s}\bar{q} \rightarrow K^\pm + \gamma e^\mp \nu_e$	9.49745×10^{-8}	9.49178×10^{-8}	2.44062×10^{-7}	3.5995×10^{-7}
$sq\bar{s}\bar{q} \rightarrow K^\pm + \gamma \mu^\mp \nu_\mu$	3.2153×10^{-5}	3.2134×10^{-5}	8.2638×10^{-5}	1.21881×10^{-4}
$ss\bar{q}\bar{q} \rightarrow K^\pm + \gamma e^\mp \nu_e$	3.5985×10^{-7}	4.01661×10^{-7}	1.3723×10^{-6}	2.22716×10^{-6}
$ss\bar{q}\bar{q} \rightarrow K^\pm + \gamma \mu^\mp \nu_\mu$	1.2183×10^{-4}	1.35381×10^{-4}	4.64623×10^{-4}	7.5405×10^{-4}

mesons, composed of quarks such as up, down, and strange quarks, the trajectories are almost linear with a slight convexity. This convexity arises from the dynamics of the light quarks and the strong force binding them, where the gluonic field predominantly influences their behavior. The small deviation from linearity is due to relativistic effects and the non-linear nature of the strong interaction at low energies. In contrast, heavy mesons, containing at least one heavy quark, exhibit concave Regge trajectories. The concavity results from the heavier quark masses dominating the system's dynamics over the gluonic field. In these mesons, the energy needed to increase spin does not correspond directly to a proportional increase in mass squared, leading to a downward-curving trajectory. Heavy quarks, moving more slowly and behaving non-relativistically, cause the meson to act more like a rigid rotor than a flexible string, further contributing to this deviation from linearity seen in light mesons [67, 111, 112]. In the present work, the tetraquark is modeled as a heavy-heavy particle-antiparticle system, following a similar Regge behavior.

Understanding Regge trajectories is essential for analyzing the hadron spectrum and offers valuable insights into the strong interaction, particularly in the non-perturbative regime of Quantum Chromodynamics (QCD). They also play a key role in predicting new particles that fit into these trajectories. The Regge trajectories in the (n, M^2) plane are plots of the principal quantum number, n , against the square of the resonance mass, M^2 . The Regge trajectories in the (n, M^2) plane are drawn for the Kaon with natural and unnatural parity states, as shown in Figs. 4a, 4b, 5a and 5b. The solid straight lines represent our calculated results. Similarly, the trajectories in the (n, M^2) plane are depicted in Figs. 6a, 6b, 7a, 7b, 8a and 8b for $ss\bar{q}\bar{q}$ and $sq\bar{s}\bar{q}$ tetraquark with various spins.

6 Results and Discussion

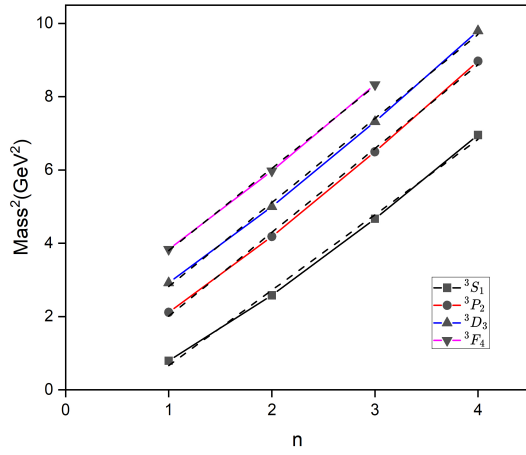
In the present work, the mass spectra of Kaon meson are calculated and tabulated in tables 1 and 2. Using the fitting parameters obtained from the kaonic mass spectrum, masses of diquarks and anti-diquarks are calculated with various color configurations. Finally, the mass spectroscopy of all strange tetraquark in a semi-relativistic and non-relativistic framework using diquark-antidiquark formalism with various possible internal structures is calculated and presented in tables 4 and 5 for antitriplet-triplet and sextet diquark-antidiquark, respectively. Table 6 shows various two-meson thresholds for different tetraquark states. In addition, the decay properties of tetraquarks in various decay channels have also been calculated. Using Fierz rearrangement, the spectator model, and heavy quarkonium annihilation, various decay channels for $T_{sq\bar{s}\bar{q}}$ and $T_{ss\bar{q}\bar{q}}$ tetraquarks are explored, which are shown in tables 7 and 10. The total decay rates for $T_{sq\bar{s}\bar{q}}$ and $T_{ss\bar{q}\bar{q}}$ strange tetraquarks are given in Table 8.

6.1 Meson

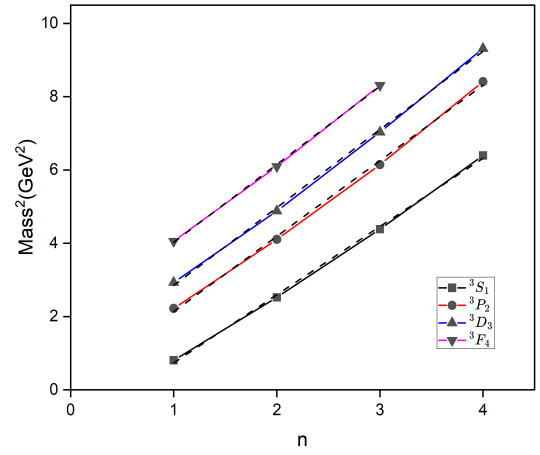
The calculated kaonic mass spectrum, when compared with various theoretical studies and with the PDG data, shows promising outcomes. For the S-wave, three resonances match the description of states calculated in the present work.

A. S – Wave

The 1^1S_0 and 3^1S_0 states in the present study match the semi-relativistic and non-relativistic state descriptions. The K^\pm are well established kaons with mass 493.77 ± 0.016 MeV, $I(J^P)$ value $\frac{1}{2}(0^-)$ and mean life 1.2380×10^{-8} s [17]. The 1^1S_0 state of the

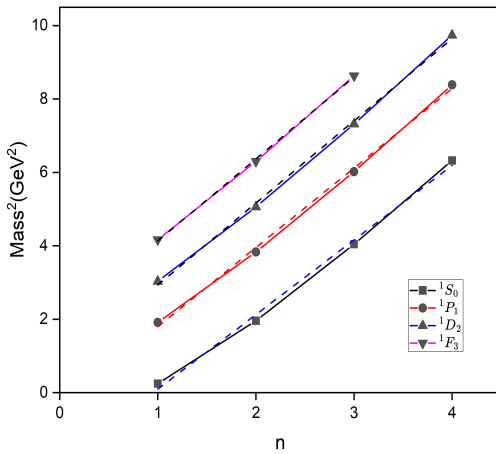


(a) Non-Relativistic formalism

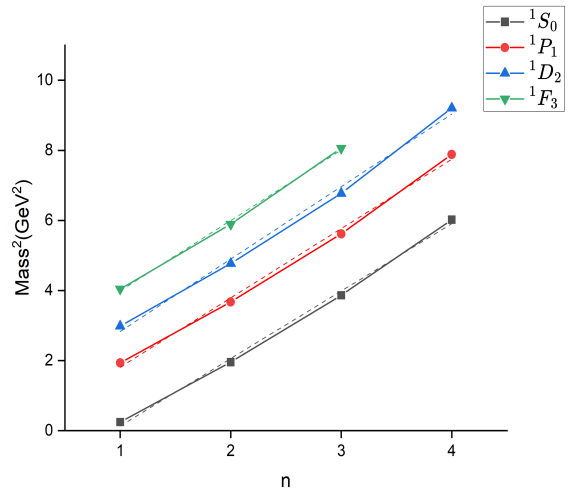


(b) Non-Relativistic formalism

Fig. 4: Regge trajectory in the (n, M^2) plane for Kaon meson with unnatural parity, (Spin $S = 0$)



(a) Non-Relativistic formalism



(b) Non-Relativistic formalism

Fig. 5: Regge trajectory in the (n, M^2) plane for Kaon meson with natural parity, (Spin $S = 1$)

present study has $I(J^P)$ value $\frac{1}{2}(0^-)$ and has a mass very close to K^\pm , 497 MeV for non-relativistic formalism and 496 for semi-relativistic formalism. The compared studies show K^\pm mass very close to the PDG value, except ref [67] and [85], which predict a mass of 30 MeV and 15 MeV lower. The $K(1830)$ resonance also has $I(J^P)$ value $\frac{1}{2}(0^-)$ and is a fair candidate for the 3^1S_0 state of present in semi-relativistic formalism. The $K(1830)$ resonance has been seen in $B^+ \rightarrow J/\psi\phi K^+$ and $18.5K^-p \rightarrow 3Kp$. process with a decay width of $168 \pm 90^{+280}_{-104}$ MeV and 250 MeV, respectively [113, 114]. This resonance has an average mass of $1874 \pm 43^{+59}_{-119}$. The masses of radially excited scalar S-wave kaons show good agreement with compared studies except ref [83], which predicts lower masses.

The vector kaon $K^*(892)$ is also a very well established state with $I(J^P)$ value $\frac{1}{2}(1^-)$ [17]. The average mass for $K^*(892)$ resonance observed in numerous hadroproduced processes including $0.9\bar{p}p \rightarrow K^+K^-\pi^0$, $8.25K^-p \rightarrow \bar{K}^0\pi^-p$, $200\pi p \rightarrow 2K_s^0X$ and $70K^+p \rightarrow K^0\pi^+X$ with an average decay width of 51.4 ± 0.8 MeV is 891.67 ± 0.26 MeV [17, 115–118]. The average mass and average decay width for $K^*(892)$ resonance observed in numerous τ lepton decay processes, including $\tau^- \rightarrow K_s\pi^- \nu_\tau$ process, are 895.5 ± 0.8 MeV and 46.2 ± 1.3 [119]. The 1^3S_1 state of the present study has mass 891 MeV and 899 MeV in non-relativistic and semi-relativistic formalism, respectively, with the $I(J^P)$ value $\frac{1}{2}(1^-)$ and fits the description of $K^*(892)$ resonance

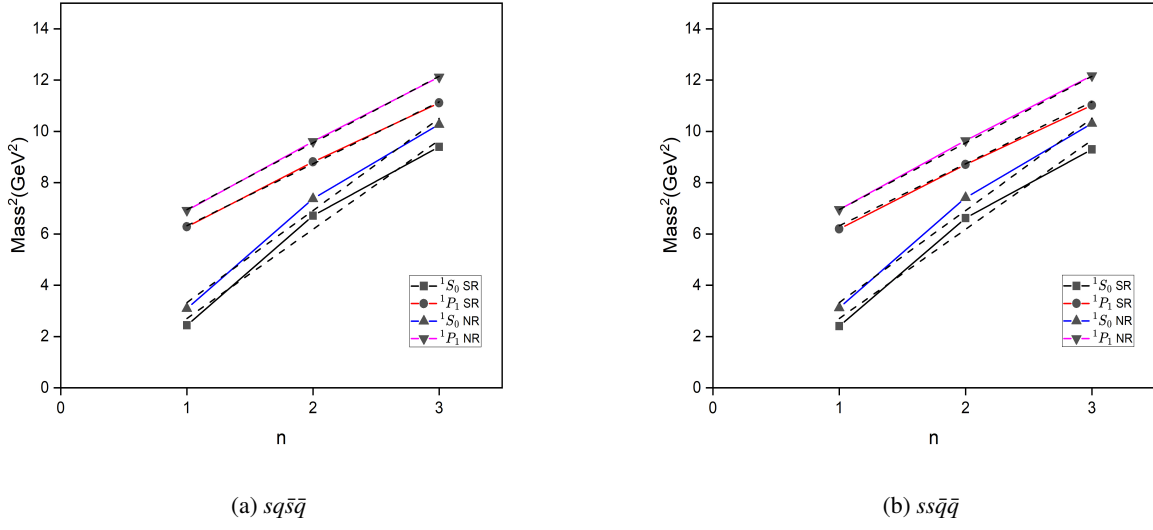


Fig. 6: Regge trajectory in the (n, M^2) plane for tetraquarks with Spin $S = 0$

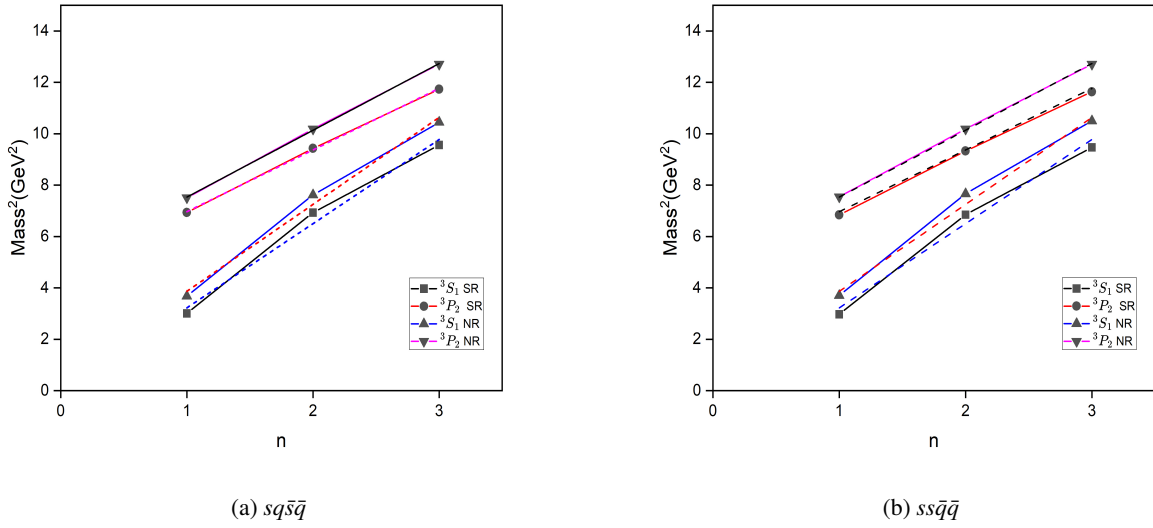


Fig. 7: Regge trajectory in the (n, M^2) plane for tetraquarks with Spin $S = 1$

very well. The mass prediction for radially excited states for the S-wave vector kaon shows similar trends with the compared theoretical studies.

B. P – Wave

The $K_1(1400)$ meson resonance has been observed in $\tau^- \rightarrow K^- \pi^+ \pi^- \nu_\tau$, $11K^- p \rightarrow \bar{K}^0 \pi^+ \pi^- n$, $8.25K^- p \rightarrow K_s^0 \pi^+ \pi^- n$, $63K^- p \rightarrow K^- 2\pi p$, $6K^- p \rightarrow \bar{K}^0 \pi^+ \pi^- n$ and $13K^\pm p \rightarrow (K\pi\pi)^{+-} p$ process with an average mass of 1403 ± 7 MeV and an average decay width of 174 ± 13 MeV. [120–125]. This resonance has the $I(J^P)$ value $\frac{1}{2}(1^+)$ and seems a reasonable fit for the 1^1P_1 state of the present study in both formalisms. The mass spectrum of radially excited states of 1^1P_1 state in the present study shows higher mass when compared with other theoretical studies except ref [83]. The mass spectrum of radial excitation of the 1^1P_1 state in ref [83] shows good agreement with the non-relativistic formalism of the present study.

The $K(1630)$ resonance has an undefined $I(J^P)$ value ($\frac{1}{2}(?)$) and has been seen in $16.0\pi^- p \rightarrow (K_s^0 \pi^+ \pi) X^+ \pi^- X^0$ with a decay width of 16_{-16}^{+19} MeV and a mass of 1629 ± 7 MeV [126]. The mass description of this state matches the 2^3P_0 state of

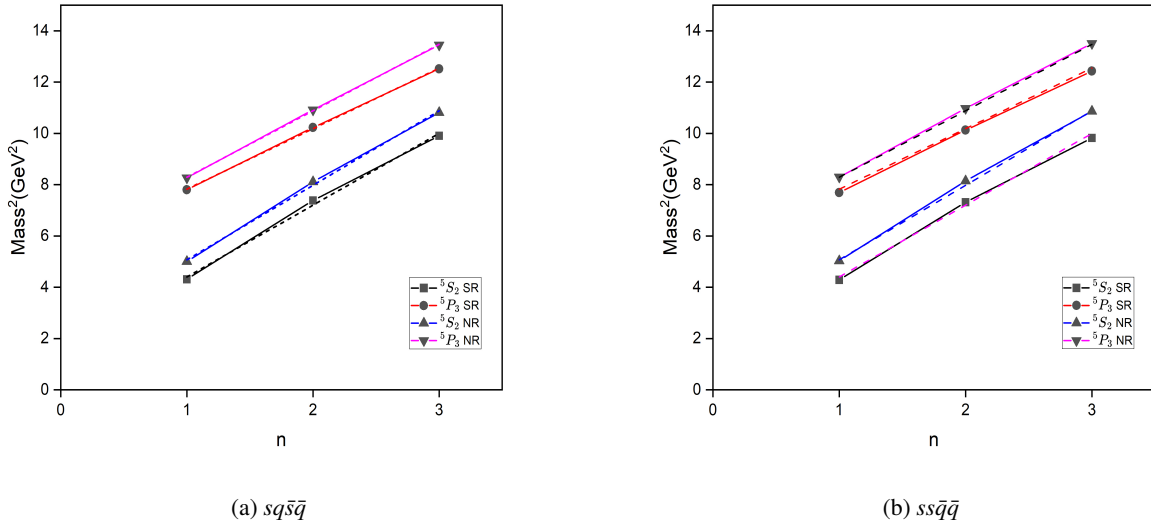


Fig. 8: Regge trajectory in the (n, M^2) plane for tetraquarks with Spin $S = 2$

the current study in semi-relativist formalism very well. In the case of radial excitation of the 3P_0 state of the present study, the ground state and first excited state predict mass lower than the compared study, while the third and fourth states predict mass near that of other studies. The ground and excited state for the 3P_1 state predicts mass higher than the compared studies, except ref [83]. The ground state of the 3P_1 state is lower in ref [83], but excited states show a comparable mass to the present study.

With an average mass of 1432.4 ± 1.3 MeV for neutral resonance and 1427.3 ± 1.5 MeV for charged resonance, the $K_2^*(1430)$ kaon resonance has $I(J^P)$ value $\frac{1}{2}(2^+)$. The neutral kaon for this resonance has been seen in $11K^-p \rightarrow K^-\pi^+n$, $11K^-p \rightarrow \bar{K}^0\pi^+\pi^-n$, $11K^-p \rightarrow \bar{K}^02\pi n$, $13K^\pm p \rightarrow pK\pi$ and $8.25K^-p \rightarrow NK_s^0\pi\pi$ process with an average decay width of 109 ± 5 [121, 122, 127–129]. Similarly, the charged $K_2^*(1430)$ kaon resonance has been seen in $J/\psi \rightarrow K^+K^-\pi^0$, $8.25K^-p \rightarrow \bar{K}^0\pi^-p$, $30K^+p \rightarrow K_s^0\pi^+p$, $50K^+p \rightarrow K_s^0\pi^+p$, $6.5K^-p \rightarrow \bar{K}^0\pi^-p$, $10K^\pm p \rightarrow K_s^0\pi p$ and $K^+p \rightarrow K^0\pi^+p$ process with an average decay rate of 100.0 ± 2.1 MeV [116, 130–134]. This state shows a good resemblance to the 1^3P_2 kaon state of the present study in semi-relativistic formalism. The $K_2^*(1980)$ kaon resonance also has $I(J^P)$ value $\frac{1}{2}(2^+)$. This resonance has an average mass of 1994_{-50}^{+60} MeV and has been seen in $\psi(2S) \rightarrow K^+K^-\eta$, $J/\psi \rightarrow K^+K^-\pi^0$ and $11K^-p \rightarrow \bar{K}^0\pi^+\pi^-n$ processes with an average decay width of 348_{-30}^{+50} MeV [28, 121, 130]. This kaonic resonance matches the description of the 2^3P_2 and 1^3F_2 state of the present study in both formalisms. The compared studies predict similar mass spectra for the ground and excited state of the 3P_2 state, except ref [67] and [85] which give a lower prediction.

C. D – Wave

The kaonic resonance $K_2(1770)$ is a well-established state with a $I(J^P)$ value of $\frac{1}{2}(2^-)$ and an average mass of 1773 ± 8 MeV. This resonance has been observed in the $B^+ \rightarrow J/\psi\phi K^+$ and $11K^-p \rightarrow K^-\omega p$ processes with an average decay width of 186 ± 14 MeV [113, 135]. This resonance is an apt candidate for the 1^1D_2 state in the non-relativistic formalism of the present study. All the compared studies, except ref [85] estimate a mass slightly few MeVs higher for the 1^1D_2 state. $K_2(2250)$ resonance also has a $I(J^P)$ value $\frac{1}{2}(2^-)$ but is not a well established particle. This state has an average mass of 2247 ± 17 MeV. been observed in the $18K^-p \rightarrow \Lambda\bar{p}X$, $8K^-p \rightarrow \Lambda\bar{p}X$ and $50K^+p \rightarrow \Lambda\bar{p}X$ processes with an average decay width of 180 ± 30 MeV [136–138]. This resonance is an excellent candidate for the 2^1D_2 and 2^3D_2 states in the non-relativistic formalism of the present study.

The $K^*(1680)$ is also a well-established particle with a $I(J^P)$ value of $\frac{1}{2}(1^-)$. This particle has an average mass of 1718 ± 18 MeV and has been seen in $B^+ \rightarrow J/\psi\phi K^+$, $11K^-p \rightarrow \bar{K}^0\pi^+\pi^-n$ and $11K^-p \rightarrow K^-\pi^+n$ processes with an average decay width of 322 ± 110 MeV [113, 121, 127]. The 1^3D_1 kaonic state in both formalisms of the present study matches the mass description of $K^*(1680)$. The $K(3100)$ resonance is a narrow peak observed in several $(\Lambda\bar{p}^+ + \text{pions})$ and $(\bar{\Lambda}p^+ + \text{pions})$ states in Σ^-Be reactions by [139] and in n and npA reactions by [140]. This state has an average mass of 3100 MeVs and an undefined $I(J^P)$ value ($??$). The 4^3D_1 state in the non-relativistic formalism of the current study is a good candidate for this kaonic resonance.

The compared studies predict the ground state for all D-wave states near the prediction for the present study. While refs. [45] and [85] predict the first radially excited D-wave state to be about 185 MeV lower, ref [83] and [67] show a much closer estimate.

Only ref [45] predicts the second and third radially excited states for D-wave kaon, which are at least a hundred MeV lower than the current study.

D. F – Wave

The $K_2^*(1980)$ meson is a well-established particle and is a pretty good fit for the 1^3F_2 state in both formalisms of the present study. The compared studies predict a higher mass value for all F-wave states by at least 100 MeVs.

F. G – Wave

As per PDG, the kaonic resonance $K_5^*(2380)$ is not a well-established particle and still needs confirmation. The $I(J^P)$ value of this state is $1\frac{1}{2}$ and has an average mass of 2382 ± 24 . This resonance has been observed in the $11K^-p \rightarrow K^- \pi^+ n$ process with an average decay of 178 ± 50 MeV [141]. The 1^3G_5 meson in the semi-relativistic formalism of the present study matches this description very well. The present study predicts that the masses of the G-wave kaonic state are lower than in the compared studies.

6.2 Tetraquark

In the present study, tetraquarks are explored as an extension of the meson concept, where a meson consists of a quark-antiquark pair. By analogy, the formalism used for calculating properties of mesons, such as mass spectra, annihilation decay rates, strong decay processes, strong decay constants, and Regge trajectories, is applied to the analysis of light-strange tetraquarks. Due to the absence of experimental data for light-strange tetraquarks from the Particle Data Group (PDG), the two-meson threshold serves as a reference point for comparison. Furthermore, since this work does not differentiate between up (u) and down (d) quarks, both isospin states $I = 0$ and $I = 1$ are taken into account in the analysis of various resonances. This approach ensures that the potential effects of isospin symmetry are not overlooked. The study also reveals that the tetraquark configuration $sq\bar{s}\bar{q}$, where q represents a light quark, has a slightly higher mass compared to the $ss\bar{q}\bar{q}$ configuration, with a difference ranging from 5 to 20 MeV in both formalism approaches. This mass difference could be indicative of the varying quark dynamics within the tetraquark system and may provide insight into the stability and decay patterns of these exotic states. Future experimental validation of these predictions will be crucial in enhancing our understanding of tetraquark structures and their role in hadron physics. In future work, we intend to integrate the isospin contribution into our examination of tetraquarks formed from light quarks.

A. S – Wave

The $f_0(1770)$ resonance has a $I(J^{PC})$ value of $0(0^{++})$ and an average mass of 1784_{-14}^{+16} MeV. This resonance has been seen in $29\pi^-p \rightarrow n\omega\phi$, $J/\psi \rightarrow \gamma\omega\phi$ and $\psi(2S) \rightarrow \gamma\pi^+\pi^-K^+K^-$ process with an average decay width of 161 ± 21 MeV [142–144]. $\pi\pi$, $K\bar{K}$, $\eta\eta$ and $\omega\phi$ decay modes of this resonance have been observed so far. This description matches very well with the 1^1S_0 state of the $ss\bar{q}\bar{q}$ and $sq\bar{s}\bar{q}$ tetraquark in $\bar{\mathbf{3}}-\mathbf{3}$ configuration within the non-relativistic formalism of the present study. If this state is considered a candidate for $f_0(1770)$ resonance, the isospin of the 1^1S_0 state can be predicted to be 0. The $f_0(1200-1600)$ resonance also has a similar $I(J^{PC})$ value but does not have a well-defined average mass. The K-matrix pole from combined analysis of $\pi^-p \rightarrow \pi^0\pi^0n$, $\pi^-p \rightarrow K\bar{K}n$ and $\bar{p}p \rightarrow \pi^0\pi^0\pi^0$, $\pi^0\eta\eta$, $\pi^0\pi^0\eta$ at rest predicts the mass of this resonance to be 1530_{-250}^{+90} with a decay width of 560 ± 40 [145]. This description makes $f_0(1200-1600)$ an ideal candidate for 1^1S_0 state of $sq\bar{s}\bar{q}$ and $ss\bar{q}\bar{q}$ tetraquark in $\bar{\mathbf{3}}-\mathbf{3}$ configuration within the semi-relativistic formalism. The X(1545) resonance has an undefined $I(J^{PC})$ value. This resonance was observed in $40\pi^-p \rightarrow K_s^0K_s^0n + m\pi^0$ with a decay width of 6.0 ± 2.5 MeV and a mass of 1545 ± 3 MeV [146]. This resonance is also an apt candidate for the 1^1S_0 state of $sq\bar{s}\bar{q}$ and $ss\bar{q}\bar{q}$ tetraquark in $\bar{\mathbf{3}}-\mathbf{3}$ configuration within the semi-relativistic formalism. All of the calculated masses for the ground state of the two tetraquarks in both formalism and internal configuration for the 1^1S_0 state are above the calculated two-meson threshold. Hence, $ss\bar{q}\bar{q}$ and $sq\bar{s}\bar{q}$ can decay strongly in two modes: $K_0^\pm + K_0^\mp$ and $\eta_s(1S) + \pi(1S)$. However, the sextet configuration for the 1^1S_0 state in non-relativistic formalism does not cross the two-meson threshold for either mode. Ref. [49, 50] calculates the mass of tetraquark nonet, predicting two tetraquark with internal structure $(qs)\bar{q}\bar{s}$, namely $a_0(980)$ and $f_0(980)$.

The $b_1(1960)$ and $h_1(1965)$ resonances have $I(J^{PC})$ values of $1(1^{+-})$ and $0(1^{+-})$ respectively. These resonances have been observed in a combined analysis of the meson channel with $I = 0, 1$ and $C = -1$ ($0.6 - 1.9p\bar{p} \rightarrow \omega\pi^0, \omega\eta\pi^0, \pi^+\pi^-$) [147]. The $b_1(1960)$ resonance has an average mass of 1960 ± 35 MeV and a decay width of 230 ± 50 MeV. The $h_1(1960)$ resonance has an average mass of 1965 ± 45 MeV and a decay width of 345 ± 75 MeV. The mass and J^{PC} value of $ss\bar{q}\bar{q}$ and $sq\bar{s}\bar{q}$ tetraquark in non-relativistic formalism with the $\bar{\mathbf{3}}-\mathbf{3}$ internal structure of the present study fit very well with those of these two resonances. If $b_1(1960)$ resonance is considered as a $ss\bar{q}\bar{q}$ or $sq\bar{s}\bar{q}$ tetraquark candidate, it can be concluded that the isospin of the considered

tetraquark is 1. Similarly, if the $h_1(1965)$ resonance is considered, the isospin can be taken as 0. The ground state of 3S_1 tetraquark has 3 decay modes for strong decay, which can be used as the two meson thresholds, namely $K_1^*(1S)K_0^\pm(1s)$, $\phi(1s)\pi(1S)$, and $\rho\eta_s$. All the calculated tetraquarks in the 1^3S_1 state lie above these two meson thresholds.

The $f_2(2010)$ resonance has an average mass of 2011_{-76}^{+62} MeV and an average decay of 202 ± 60 MeV. This resonance is a well-established particle with a $I(J^{PC})$ value of $0(2^{++})$ and has been observed in the $22\pi^-p \rightarrow \phi\phi n$ process [148]. The 1^5S_2 tetraquark in the semi-relativistic formalism of the present study fits very well with this description; however, numerous studies predict this resonance as a strangeonium state.

In the case of the 1^5S_2 state of tetraquark in non-relativistic formalism, five resonances ($X(2210)$, $X_2(2210)$, $f_J(2220)$, $f_2(2240)$ and $a_2(2255)$) show great resemblance. The $I(J^{PC})$ values of $X_2(2210)$, $f_2(2240)$ and $a_2(2255)$ resonances are $0(2^{++})$, $0(2^{++})$ and $1(2^{++})$ respectively. The $X(2210)$ resonance has an undefined $I(J^{PC})$ value, while the $f_J(2220)$ resonance has a half-defined $0(2^{++}$ or $4^{++})$. The $f_J(2220)$ resonance has been seen in $e^+e^- \rightarrow J/\psi \rightarrow \gamma\pi^+\pi^-$, $e^+e^- \rightarrow J/\psi \rightarrow \gamma K^+K^-$, $e^+e^- \rightarrow J/\psi \rightarrow \gamma K_s^0 K_s^0$, $e^+e^- \rightarrow J/\psi \rightarrow \gamma p\bar{p}$, $e^+e^- \rightarrow \gamma K^+K^-$, $e^+e^- \rightarrow \gamma K_s^0 K_s^0$ and $11K^-p \rightarrow K^+K^-\Lambda$ process with an average decay width of 23_{-7}^{+8} MeV and an average mass of 2231.1 ± 3.5 MeV [149–151]. The $X(2210)$ resonance has been observed in the $10\pi^-p \rightarrow K^+K^-n$ and $11.2\pi^-p$ processes with a mass of 2210_{-21}^{+79} MeV and 2207 ± 22 MeV, respectively [152, 153]. The decay widths of the $10\pi^-p \rightarrow K^+K^-n$ and $11.2\pi^-p$ processes are estimated to be 203_{-87}^{+437} MeV and 130 MeV, respectively. $X_2(2210)$ has been observed in the fit of tensor partial waves from BES3 in the multipole basis, which might be a cluster of $J^{PC} = 2^{++}$ resonances [154]. This resonance was observed in the $J/\psi \rightarrow \gamma\pi^0\pi^0$, $\gamma K_s^0 K_s^0$ process while searching tensor glueball. The $X_2(2210)$ has an average mass of 2210 ± 60 and a decay width of 360 ± 120 MeV. The $f_2(2240)$ resonance has been observed in the combined analysis of [155–160] with an average mass of 2240 ± 15 and a decay width of 241 ± 30 MeV. The partial wave analysis of $\bar{p}p \rightarrow \eta\eta\pi^0$ done in the combined analysis of [155, 161–163] predicts the $a_2(2255)$ resonance, which has an average mass of 2255 ± 20 MeV and a decay width of 230 ± 15 MeV. The mass of the 1^5S_2 state of $sq\bar{q}\bar{q}$ and $sq\bar{s}\bar{q}$ tetraquarks in non-relativistic formalism is 2243.27 and 2236.40 MeV, which makes its mass adjacent to all the resonances discussed so far. If the tetraquark is assigned isospin $I = 1$, then $a_2(2255)$ resonance is the appropriate choice. However, if the tetraquark is assigned a zero isospin, then $f_J(2220)$ and $f_2(2240)$ resonance are fair candidates.

B. P – Wave

The $\eta(2190)$ resonance has been observed in the broad $J^P = 0^-$ meson in J/ψ radiative decays with an average mass of 2190 ± 50 MeV and a decay width of 850 ± 100 MeV [164]. This resonance is not a well-established particle but has a $I(J^{PC})$ value of $0(0^{-+})$. This description matches the 1^3P_0 state $sq\bar{s}\bar{q}$ and $ss\bar{q}\bar{q}$ tetraquark in semi-relativistic formalism, which have masses of 2147 MeV and 2133 MeV, respectively.

The $\eta(2320)$ resonance was seen by the combined analysis of $\bar{p}p \rightarrow \eta\eta\eta$ from [165] and $\bar{p}p \rightarrow \eta\pi^0\pi^0$ from [160] with a mass of 2320 ± 15 MeV and a decay width of 230 ± 35 MeV. The $I(J^{PC})$ value of this resonance is $0(0^{-+})$. The masses of 1^3P_0 state $sq\bar{s}\bar{q}$ and $ss\bar{q}\bar{q}$ tetraquark in non-relativistic formalism have masses of 2305 MeV and 2315 MeV respectively, which make them an ideal candidate for this resonance. The $\pi(2360)$ resonance has been enhanced by the partial wave analysis of $p\bar{p}$ annihilation channels in flight with $I = 1$ and $C = +1$ with a decay width of 300_{-50}^{+100} in $2.0\bar{p}p \rightarrow 3\pi^0$, $\pi^0\eta$, $\pi^0\eta'$ processes [162]. The mass and $I(J^{PC})$ value of this resonance are 2360 ± 25 and $1(0^{-+})$, respectively. These values also match the 1^3P_0 state $sq\bar{s}\bar{q}$ and $ss\bar{q}\bar{q}$ tetraquark in non-relativistic formalism.

The 2^3P_0 state $sq\bar{s}\bar{q}$ and $ss\bar{q}\bar{q}$ tetraquark in semi-relativistic formalism with $\mathbf{6} - \bar{\mathbf{6}}$ The color structure has four resonances as potential candidates, namely, $\eta(2010)$, $\pi(2070)$, $\eta(2100)$ and $X(2100)$. The $\eta(2010)$ has an average mass of 2010_{-60}^{+35} MeV and a decay width of 270 ± 60 MeV. The $\pi(2070)$ was observed along with the $\pi(2360)$ resonance mentioned before with the same decay width and a mass of 2070 ± 35 . The $\eta(2100)$ resonance has been observed in two different processes. When derived from a partial wave analysis of $J/\psi \rightarrow \gamma\phi\phi$, for which the primary signal is $\eta(2225) \rightarrow \phi\phi$, the $\eta(2100)$ resonance is observed in $J/\psi \rightarrow \gamma K^+K^-K^+K^-$ with mass 2050_{-24-26}^{+30+75} MeV and decay width $250_{-30-164}^{+36+181}$ MeV [166]. However, when seen in the $J/\psi \rightarrow 4\pi\gamma$ process, the $\eta(2100)$ resonance has an average mass of 2103 ± 50 MeV and a decay width of 187 ± 75 MeV [167]. The $X(2100)$ resonance was seen in the $100\pi^-p \rightarrow 2\eta X$ process with a mass 2100 ± 40 MeV and a decay width of 250 ± 40 MeV [168]. The $I(J^{PC})$ value for $\eta(2100)$ and $\eta(2010)$ is $0(0^{-+})$ and suggests the tetraquark has an isospin 0. On the other hand, $\pi(2070)$ has a $I(J^{PC})$ value of $1(0^{-+})$, suggesting the tetraquark's isospin zero. The 2^3P_0 state $sq\bar{s}\bar{q}$ and $ss\bar{q}\bar{q}$ tetraquark in semi-relativistic formalism with $\mathbf{6} - \bar{\mathbf{6}}$ color structure in the present study has masses of 2084 MeV and 2070 MeV, respectively. The four resonances match the description of 2^3P_0 states very well, making them potential candidates.

The 1^5P_1 state $sq\bar{s}\bar{q}$ and $ss\bar{q}\bar{q}$ tetraquark in non-relativistic formalism suffer the same fate as the 2^3P_0 state and the 1^5S_2 state with multiple resonances as potential candidates. The 1^5P_1 has a mass of 2304 MeV and 2314 MeV for $sq\bar{s}\bar{q}$ and $ss\bar{q}\bar{q}$ tetraquark in non-relativistic formalism, respectively, with a J^{PC} value of 1^{--} . The $\rho(2270)$ resonance has been seen in $0.6 - 1.9\bar{p}p \rightarrow \omega\pi^0$, $\omega\eta\pi^0$, $\pi^+\pi^-$ with a mass of 2265 ± 40 MeV and decay width of 325 ± 80 MeV [147]. When observed in the $20 - 70\gamma p \rightarrow p\omega\pi^+\pi^-\pi^0$ process, the $\rho(2265)$ resonance has a mass prediction of 2280 ± 50 and a decay width of 440 ± 110 MeV [169]. The partial wave analysis of the data on $p\bar{p} \rightarrow \bar{\Lambda}\Lambda$ from [170] predicts the mass and decay width of $\omega(2290)$ resonance to be 2290 ± 20 MeV and 275 ± 35 respectively [171]. Similarly, the photon diffractive dissociation to $\rho\rho\pi$ and $\rho\pi\pi\pi$

states in $25 - 50\gamma p \rightarrow \rho^\pm \rho^0 \pi^\mp$ predicts the $\omega(2330)$ resonance with a mass of 2330 ± 30 MeV and a decay width of 435 ± 75 MeV [172]. Considering the calculated masses and J^{PC} of 1^3P_1 state $sq\bar{s}\bar{q}$ and $ss\bar{q}\bar{q}$ tetraquark, the resonances discussed here contest as potential candidates. If the resonances $\omega(2290)$ and $\omega(2230)$ are considered, the tetraquark must have isospin zero since their $I(J^{PC})$ value is $0(1^{--})$. However, considering $\rho(2265)$ as a tetraquark candidate suggests the tetraquark with isospin 1, given that the $I(J^{PC})$ of $\rho(2265)$ is $1(1^{--})$.

The 1^3P_1 state $sq\bar{s}\bar{q}$ and $ss\bar{q}\bar{q}$ tetraquark in semi-relativistic formalism for the present study has 2153 MeV and 2139 MeV, respectively. The $\rho(2150)$ resonance is a not well-established resonance that was earlier referred to as $T_1(2190)$ [17]. This resonance has been seen in numerous e^+e^- processes [28, 29, 173], $p\bar{p} \rightarrow \pi\pi$ process [174, 175], S-channel $N\bar{N}$ process [147, 176] and $\pi^-p \rightarrow \omega\pi^0n$ process [177, 178]. No average mass is available in PDG but 2150 MeV can be taken as the central value for its mass. This state has a $I(J^{PC})$ value of $1(1^{--})$, which suggests that this resonance can be a good tetraquark candidate with isospin 1. Ref. [55, 56] speculates $Y(2175)$ as a light vector tetraquark state with a mass of 2173 ± 85 MeV and a decay width of 91.1 ± 20.5 MeV, with a strong emphasis on the internal structure of the resonance being $[su][\bar{s}\bar{u}]$. Similarly, ref. [53] and [54] predict an explanation of the P-wave mass of light strange vector tetraquark state between 2.06 ± 0.13 GeV and 3.52 ± 0.11 GeV for the P-wave with partial derivative and 2.06 ± 0.13 GeV to 3.54 ± 0.09 GeV for the P-wave with covariant derivative. Ref. [54] predicts $Y(2175)$, $X(2240)$ and $X(2400)$ as tetraquark candidates.

$X(2600)$ resonance has undefined $I(J^{PC})$ value and is seen in $J/\psi \rightarrow \gamma\pi^+\pi^-\eta'$ process with an average mass and decay width of $2618.3 \pm 2.0_{-1.4}^{+16.3}$ MeV and $195 \pm 5_{-17}^{+26}$ MeV [179]. This resonance has been observed to decay in $f_0(1500)\eta'$ mode and $X(1540)\eta'$ mode, making a very possible candidate for $ss\bar{q}\bar{q}$ and $sq\bar{s}\bar{q}$ tetraquark. Since it has an undefined J^{PC} value, it becomes very difficult to point out the exact state of this resonance. However, it is safe to predict that this resonance is a P-wave state.

7 Conclusion

To summarize, utilizing fitting parameters determined from Kaon mass spectra in a semi-relativistic and non-relativistic framework, we have calculated the mass spectra of $sq\bar{s}\bar{q}$ and $ss\bar{q}\bar{q}$ tetraquarks in different diquark-antidiquark configurations and internal structures, including relativistic corrections. The computed states have corresponding J^{PC} values assigned to them. Furthermore, we have used the annihilation model [41], spectator model [92, 93], and rearrangement model [108] to analyze the decay processes of Kaons and $sq\bar{s}\bar{q}$ and $ss\bar{q}\bar{q}$ tetraquarks. Additionally, we have determined two-meson thresholds in both formalisms for tetraquarks. For various spins and parity states, regge plots for Kaon states and strange tetraquarks have been plotted.

Various resonances have been investigated as potential candidates for S-wave Kaon states, including $K(497)$, $K(1830)$, and $K_1^*(891)$. For P-wave Kaon states, we examined $K_1(1400)$, $K(1630)$, $K_2^*(1430)$, and $K_2^*(1980)$. D-wave candidates like $K_2(1770)$, $K_2(2250)$, $K^*(1680)$, $K(3100)$, and $K_2(2250)$ were explored, along with $K_2^*(1980)$ as an F-wave candidate and $K_5^*(2380)$ as a G-wave candidate. For S-wave tetraquark states $ss\bar{q}\bar{q}$ and $sq\bar{s}\bar{q}$, potential candidates include $f_0(1770)$, $X(1545)$, $b_1(1960)$, $h_1(1965)$, $f_2(2010)$, $X(2210)$, $X_2(2210)$, $f_J(2220)$, $f_2(2240)$, and $a_2(2255)$. Similarly, potential P-wave candidates such as $\eta(2190)$, $\eta(2320)$, $\pi(2360)$, $\eta(2100)$, $\eta(2010)$, $\pi(2070)$, $X(2100)$, $\rho(2270)$, $\rho(2265)$, $\omega(2290)$, $\omega(2330)$, $\rho(2150)$, and $X(2600)$ resonances were explored.

These findings could potentially serve as valuable input and comparative data for institutions such as PANDA, J-PARC, Belle, LHCb, and others that focus on in-depth analyses of resonances involving strange quarks. This investigation provides a robust foundation for future studies employing the formalism described here to investigate tetraquarks with various quark flavors. Additionally, this research paves the way for more comprehensive theoretical models and experimental validations, thereby enhancing our understanding of hadronic structures and interactions. The methodologies and results presented could also contribute to the development of new experimental techniques and the refinement of existing ones, facilitating more precise measurements and discoveries in the field of particle physics.

8 Data Availability Statement

The datasets generated during and/or analysed during the current study are available from the corresponding author on reasonable request.

References

1. M. Gell-Mann, Phys. Lett. **8**, 214-215 (1964)
2. S. K. Choi *et al.* [Belle], Phys. Rev. Lett. **91**, 262001 (2003)
3. R. L. Jaffe, Phys. Rev. Lett. **38**, 195-198 (1977) [erratum: Phys. Rev. Lett. **38**, 617 (1977)]
4. R. L. Jaffe, Phys. Rev. D **15**, 267 (1977)
5. D. B. Lichtenberg, E. Predazzi, D. H. Weingarten and J. G. Wills, Phys. Rev. D **18**, 2569 (1978)
6. C. Gignoux, B. Silvestre-Brac and J. M. Richard, Phys. Lett. B **193**, 323 (1987)

7. M. Wagner, A. Abdel-Rehim, C. Alexandrou, M. Dalla Brida, M. Gravina, G. Koutsou, L. Scorzato and C. Urbach, *J. Phys. Conf. Ser.* **503**, 012031 (2014)
8. W. Chen, H. X. Chen, X. Liu, T. G. Steele and S. L. Zhu, *Phys. Lett. B* **773**, 247-251 (2017)
9. Z. Ghalenovi and M. M. Sorkhi, *Eur. Phys. J. Plus* **135**, no.5, 399 (2020)
10. S. Noh and W. Park, *Phys. Rev. D* **108**, no.1, 014004 (2023)
11. H. Mutuk, *Eur. Phys. J. C* **83**, no.5, 358 (2023)
12. P. G. Ortega, J. Segovia, D. R. Entem and F. Fernandez, *Phys. Lett. B* **841**, 137918 (2023) [erratum: *Phys. Lett. B* **847**, 138308 (2023)]
13. A. Esposito, A. Pilloni and A. D. Polosa, *Phys. Rept.* **668**, 1-97 (2017)
14. A. Ali, J. S. Lange and S. Stone, *Prog. Part. Nucl. Phys.* **97**, 123-198 (2017)
15. S. L. Olsen, T. Skwarnicki and D. Zieminska, *Rev. Mod. Phys.* **90**, no.1, 015003 (2018)
16. R. F. Lebed, R. E. Mitchell and E. S. Swanson, *Prog. Part. Nucl. Phys.* **93**, 143-194 (2017)
17. R. L. Workman *et al.* [Particle Data Group], *PTEP* **2022**, 083C01 (2022)
18. H. X. Chen, W. Chen, X. Liu, Y. R. Liu and S. L. Zhu, *Rept. Prog. Phys.* **86**, no.2, 026201 (2023)
19. S. K. Choi *et al.* [Belle], *Phys. Rev. Lett.* **100**, 142001 (2008)
20. N. Mahajan, *Phys. Lett. B* **679**, 228-230 (2009)
21. V. M. Abazov *et al.* [D0], *Phys. Rev. Lett.* **117**, no.2, 022003 (2016)
22. M. Ablikim *et al.* [BESIII], *Phys. Rev. Lett.* **110**, 252001 (2013)
23. R. Aaij *et al.* [LHCb], *Sci. Bull.* **65**, no.23, 1983-1993 (2020)
24. A. Poluektov *et al.* [Belle], *Phys. Rev. D* **81**, 112002 (2010)
25. R. Aaij *et al.* [LHCb], *Phys. Rev. D* **95**, no.1, 012002 (2017)
26. R. Aaij *et al.* [LHCb], *Phys. Rev. Lett.* **127**, no.8, 082001 (2021)
27. B. Aubert *et al.* [BaBar], *Phys. Rev. D* **78**, 034023 (2008)
28. M. Ablikim *et al.* [BESIII], *Phys. Rev. D* **101**, no.3, 032008 (2020)
29. M. Ablikim *et al.* [BESIII], *Phys. Rev. D* **103**, no.7, 072007 (2021)
30. J. P. Lees *et al.* [BaBar], *Phys. Rev. D* **101**, no.1, 012011 (2020)
31. B. Singh *et al.* [PANDA], *Phys. Rev. D* **95**, no.3, 032003 (2017)
32. B. Singh *et al.* [PANDA], *Eur. Phys. J. A* **52**, no.10, 325 (2016)
33. B. Singh [PANDA], *Nucl. Phys. A* **954**, 323-340 (2016)
34. B. Singh, W. Erni, B. Krusche, M. Steinacher, N. Walford, B. Liu, H. Liu, Z. Liu, X. Shen and C. Wang, *et al.* *J. Phys. G* **46**, no.4, 045001 (2019)
35. G. Barucca *et al.* [PANDA], *Eur. Phys. J. A* **55**, no.3, 42 (2019)
36. V. Abazov *et al.* [PANDA], [arXiv:2304.11977 [nucl-ex]].
37. G. Barucca *et al.* [PANDA], *Eur. Phys. J. A* **57**, no.6, 184 (2021)
38. K. Aoki, H. Fujioka, T. Gogami, Y. Hidaka, E. Hiyama, R. Honda, A. Hosaka, Y. Ichikawa, M. Ieiri and M. Isaka, *et al.* [arXiv:2110.04462 [nucl-ex]].
39. V. Kher, N. Devlani and A. K. Rai, *Chin. Phys. C* **41**, no.7, 073101 (2017)
40. A. K. Rai, B. Patel and P. C. Vinodkumar, *Phys. Rev. C* **78**, 055202 (2008)
41. V. Kher and A. K. Rai, *Chin. Phys. C* **42**, no.8, 083101 (2018)
42. K. R. Purohit, P. Jakhad and A. K. Rai, *Phys. Scripta* **97**, no.4, 044002 (2022)
43. C. Menapara and A. K. Rai, *Int. J. Mod. Phys. A* **38**, no.09n10, 2350053 (2023)
44. R. Chaturvedi and A. K. Rai, *Eur. Phys. J. A* **58**, no.11, 228 (2022)
45. J. Oudichhya, K. Gandhi and A. K. Rai, *Phys. Rev. D* **108**, no.1, 014034 (2023)
46. V. Kher, N. Devlani and A. K. Rai, *Chin. Phys. C* **41**, no.9, 093101 (2017)
47. C. Menapara and A. K. Rai, *Int. J. Mod. Phys. A* **37**, no.27, 2250177 (2022)
48. A. K. Rai, J. N. Pandya and P. C. Vinodkumar, *Indian J. Phys. A* **80**, 387-392 (2006) [arXiv:hep-ph/0603008 [hep-ph]].
49. H. Kim and K. S. Kim, *EPJ Web Conf.* **291**, 02002 (2024)
50. H. Kim and K. S. Kim, [arXiv:2403.18411 [hep-ph]].
51. S. Acharya *et al.* [ALICE], [arXiv:2312.12830 [hep-ex]].
52. E. Santopinto and G. Galata, *Phys. Rev. C* **75**, 045206 (2007)
53. Z. G. Wang and S. L. Wan, *Chin. Phys. Lett.* **23**, 3208-3210 (2006)
54. Q. Xin and Z. G. Wang, *Chin. Phys. C* **48**, no.3, 033104 (2024)
55. S. Agaev, K. Azizi and H. Sundu, *Turk. J. Phys.* **44**, no.2, 95-173 (2020)
56. S. S. Agaev, K. Azizi and H. Sundu, *Phys. Rev. D* **101**, no.7, 074012 (2020)
57. C. Lodha and A. K. Rai, *Few Body Syst.* **65**, no.4, 99 (2024)
58. C. Lodha and A. K. Rai, *Eur. Phys. J. Plus* **139**, no.7, 663 (2024)
59. C. Lodha, J. Oudichhya, R. Tiwari and A. K. Rai, *Journal of Condensed Matter* **1**, no.02, 105-109 (2023)
60. R. Tiwari, D. P. Rathaud and A. K. Rai, *Eur. Phys. J. A* **57**, no.10, 289 (2021)
61. R. Tiwari, D. P. Rathaud and A. K. Rai, *Indian J. Phys.* **97**, no.3, 943-954 (2023)

62. W. Lucha and F. F. Schoberl, [arXiv:hep-ph/9601263 [hep-ph]].
63. N. Devlani and A. K. Rai, Phys. Rev. D **84**, 074030 (2011)
64. S. F. Radford, W. W. Repko and M. J. Saelim, Phys. Rev. D **80**, 034012 (2009) doi:10.1103/PhysRevD.80.034012
65. E. Eichten, K. Gottfried, T. Kinoshita, K. D. Lane and T. M. Yan, Phys. Rev. D **21**, 203 (1980)
66. C. Quigg and J. L. Rosner, Phys. Rept. **56**, 167-235 (1979)
67. S. Godfrey and N. Isgur, Phys. Rev. D **32**, 189-231 (1985)
68. N. Brambilla, A. Pineda, J. Soto and A. Vairo, Phys. Rev. D **63**, 014023 (2001) doi:10.1103/PhysRevD.63.014023
69. Y. Koma, M. Koma and H. Wittig, Phys. Rev. Lett. **97**, 122003 (2006)
70. W. Lucha, F. F. Schoberl and D. Gromes, Phys. Rept. **200**, 127-240 (1991)
71. M. B. Voloshin, Prog. Part. Nucl. Phys. **61**, 455-511 (2008)
72. V. R. Debastiani and F. S. Navarra, Chin. Phys. C **43**, no.1, 013105 (2019)
73. P. Lundhammar and T. Ohlsson, Phys. Rev. D **102**, no.5, 054018 (2020)
74. H. A. Bethe and E. E. Salpeter, "Quantum Mechanics of One- and Two-Electron Atoms," 1957, doi:10.1007/978-3-662-12869-5
75. S. Patel and P. C. Vinodkumar, Eur. Phys. J. C **76**, no.7, 356 (2016) doi:10.1140/epjc/s10052-016-4186-6 [arXiv:1606.01047 [hep-ph]].
76. L. H. Thomas, Nature **117**, 514 (1926)
77. B. Delamotte, Am. J. Phys. **72**, 170-184 (2004)
78. C. Cohen-Tannoudji, B. Diu, and F. Laloe, Quantum Mechanics, Vol. 2, Wiley-VHC (1978).
79. Debastiani, V. R. (2016). Espectroscopia do Todo-Charme Tetraquark. Master's Dissertation, Instituto de Física, University of São Paulo, São Paulo.
80. D. Ebert, R. N. Faustov, V. O. Galkin and W. Lucha, Phys. Rev. D **76**, 114015 (2007)
81. S. Fredriksson and M. Jandel, Phys. Rev. Lett. **48**, 14 (1982)
82. W. Park and S. H. Lee, Nucl. Phys. A **925**, 161-184 (2014)
83. S. Ishida and K. Yamada, Phys. Rev. D **35**, 265 (1987)
84. J. Vijande, F. Fernandez and A. Valcarce, J. Phys. G **31**, 481 (2005)
85. D. Ebert, R. N. Faustov and V. O. Galkin, Phys. Rev. D **79**, 114029 (2009)
86. P. Maris, Few Body Syst. **32**, 41-52 (2002)
87. R. N. Faustov, V. O. Galkin and E. M. Savchenko, Universe **7**, no.4, 94 (2021)
88. J. K. Chen, J. Q. Xie, X. Feng and H. Song, Eur. Phys. J. C **83**, no.12, 1133 (2023)
89. J. Ferretti, Few Body Syst. **60**, no.1, 17 (2019)
90. P. L. Yin, Z. F. Cui, C. D. Roberts and J. Segovia, Eur. Phys. J. C **81**, no.4, 327 (2021)
91. M. Hess, F. Karsch, E. Laermann and I. Wetzorke, Phys. Rev. D **58**, 111502 (1998)
92. C. Becchi, A. Giachino, L. Maiani and E. Santopinto, Phys. Lett. B **806**, 135495 (2020)
93. C. Becchi, J. Ferretti, A. Giachino, L. Maiani and E. Santopinto, Phys. Lett. B **811**, 135952 (2020)
94. J. Segovia, P. G. Ortega, D. R. Entem and F. Fernández, Phys. Rev. D **93**, no.7, 074027 (2016)
95. W. Kwong, P. B. Mackenzie, R. Rosenfeld and J. L. Rosner, Phys. Rev. D **37**, 3210 (1988)
96. W. Kwong and J. L. Rosner, Phys. Rev. D **38**, 279 (1988)
97. G. Belanger and P. Moxhay, Phys. Lett. B **199**, 575-579 (1987)
98. C. Lodha and A. K. Rai, PoS **HQL2023**, 073 (2024)
99. G. L. Wang and X. G. Wu, Chin. Phys. C **44**, no.6, 063104 (2020)
100. D. Ebert, R. N. Faustov and V. O. Galkin, Phys. Lett. B **635**, 93-99 (2006) doi:10.1016/j.physletb.2006.02.042 [arXiv:hep-ph/0602110 [hep-ph]].
101. R. Van Royen and V. F. Weisskopf, Nuovo Cim. A **50**, 617-645 (1967)
102. N. V. Drenska, R. Faccini and A. D. Polosa, Phys. Lett. B **669**, 160-166 (2008)
103. Y. W. Jiang, W. H. Tan, H. X. Chen and E. L. Cui,
104. S. S. Agaev, K. Azizi, B. Barsbay and H. Sundu, Nucl. Phys. A **1041**, 122768 (2024)
105. S. S. Agaev, K. Azizi, B. Barsbay and H. Sundu, Phys. Lett. B **844**, 138089 (2023)
106. S. S. Agaev, K. Azizi, B. Barsbay and H. Sundu, Eur. Phys. J. Plus **138**, no.10, 935 (2023)
107. Q. F. Lü, K. L. Wang and Y. B. Dong, Chin. Phys. C **44**, no.2, 024101 (2020)
108. A. Ali, L. Maiani and A. D. Polosa, Cambridge University Press, 2019, ISBN 978-1-316-76146-5, 978-1-107-17158-9, 978-1-316-77419-9
109. M. x. Luo, K. Wang, T. Xu, L. Zhang and G. Zhu, Phys. Rev. D **93**, no.5, 055042 (2016)
110. V. B. Berestetskii, E. M. Lifshitz and L. P. Pitaevskii, Pergamon Press, 1982,
111. P. D. B. Collins, Cambridge University Press, 2023, ISBN 978-1-109-40326-9, 978-1-109-40329-0, 978-1-109-40328-3, 978-0-521-11035-8 doi:10.1017/9781009403269
112. V. V. Anisovich, Phys. Usp. **47**, 45-67 (2004) doi:10.1070/PU2004v047n01ABEH001333
113. R. Aaij *et al.* [LHCb], Phys. Rev. Lett. **118**, no.2, 022003 (2017)
114. T. Armstrong *et al.* [Bari-Birmingham-CERN-Milan-Paris-Pavia], Nucl. Phys. B **221**, 1-15 (1983)

115. M. Albrecht *et al.* [Crystal Barrel], *Eur. Phys. J. C* **80**, no.5, 453 (2020)
116. M. Baubillier *et al.* [Birmingham-CERN-Glasgow-Michigan State-Paris], *Z. Phys. C* **26**, 37 (1984)
117. A. Napier, J. Schneps, T. Y. Chen, E. W. Jenkins, K. W. Lai, J. LeBritton, Y. C. Lin, A. E. Pifer, H. C. Fenker and D. R. Green, *et al. Phys. Lett. B* **149**, 514 (1984)
118. M. Barth *et al.* [Brussels-Genoa-Mons-Nijmegen-Serpukhov-CERN], *Nucl. Phys. B* **223**, 296 (1983) [erratum: *Nucl. Phys. B* **232**, 547 (1984)]
119. D. Epifanov *et al.* [Belle], *Phys. Lett. B* **654**, 65-73 (2007)
120. D. M. Asner *et al.* [CLEO], *Phys. Rev. D* **62**, 072006 (2000)
121. D. Aston, N. Awaji, J. D'Amore, W. Dunwoodie, R. Endorf, K. Fujii, H. Hayashii, S. Iwata, W. B. Johnson and R. Kajikawa, *et al. Nucl. Phys. B* **292**, 693 (1987)
122. M. Baubillier *et al.* [BIRMINGHAM-CERN-GLASGOW-MICHIGAN STATE-PARIS], *Nucl. Phys. B* **202**, 21-42 (1982)
123. C. Daum *et al.* [ACCMOR], *Nucl. Phys. B* **187**, 1-41 (1981)
124. A. Etkin, K. J. Foley, J. H. Goldman, R. S. Longacre, W. A. Love, T. W. Morris, S. Ozaki, E. D. Platner, A. C. Saulys and C. D. Wheeler, *et al. Phys. Rev. D* **22**, 42-60 (1980)
125. R. K. Carnegie, R. J. Cashmore, M. Davier, W. M. Dunwoodie, T. A. Lasinski, D. W. G. S. Leith and S. H. Williams, *Nucl. Phys. B* **127**, 509-517 (1977)
126. V. M. Karnaukhov, V. I. Moroz and C. Coca, *Phys. Atom. Nucl.* **61**, 203-206 (1998)
127. D. Aston, N. Awaji, T. Bienz, F. Bird, J. D'Amore, W. Dunwoodie, R. Endorf, K. Fujii, H. Hayashi and S. Iwata, *et al. Nucl. Phys. B* **296**, 493-526 (1988)
128. D. Aston, R. K. Carnegie, W. M. Dunwoodie, S. Durkin, P. Estabrooks, R. J. Hemingway, A. Honma, D. Hutchinson, W. B. Johnson and P. F. Kunz, *et al. Nucl. Phys. B* **247**, 261-292 (1984)
129. P. Estabrooks, R. K. Carnegie, A. D. Martin, W. M. Dunwoodie, T. A. Lasinski and D. W. G. S. Leith, *Nucl. Phys. B* **133**, 490-524 (1978)
130. M. Ablikim *et al.* [BESIII], *Phys. Rev. D* **100**, no.3, 032004 (2019)
131. W. E. Cleland, A. Delfosse, P. A. Dorsaz, J. L. Gloor, M. N. Kienzle-Focacci, G. Mancarella, A. D. Martin, M. Martin, P. Muhlemann and C. Nef, *et al. Nucl. Phys. B* **208**, 189-227 (1982)
132. S. Toaff, B. Musgrave, J. J. Phelan, P. Schultz, R. Smith, A. J. Snyder, R. Ammar, R. Davis, C. Eklund and L. Herder, *et al. Phys. Rev. D* **23**, 1500-1513 (1981)
133. A. D. Martin, T. Shimada, R. Baldi, T. Bohringer, P. A. Dorsaz, V. Hungerbuhler, M. N. Kienzle-Focacci, M. Martin, A. Mermoud and C. Nef, *et al. Nucl. Phys. B* **134**, 392-412 (1978)
134. K. W. J. Barnham, D. C. Colley, M. Jobes, K. Pathak, L. Riddiford, P. M. Watkins, I. Griffiths, I. S. Hughes, I. McLaren and C. D. Procter, *et al. Nucl. Phys. B* **28**, 171-183 (1971)
135. D. Aston, T. Bienz, F. Bird, W. Dunwoodie, W. Johnson, P. F. Kunz, Y. Kwon, D. W. G. S. Leith, L. Levinson and B. Ratcliff, *et al. Phys. Lett. B* **308**, 186-192 (1993)
136. T. Armstrong *et al.* [Bari-Birmingham-CERN-Milan-Paris-Pavia], *Nucl. Phys. B* **227**, 365-386 (1983)
137. M. Baubillier *et al.* [Birmingham-CERN-Glasgow-Michigan State-Paris], *Nucl. Phys. B* **183**, 1-11 (1981)
138. W. E. Cleland, A. Delfosse, P. A. Dorsaz, J. L. Gloor, M. N. Kienzle-Focacci, G. Mancarella, A. D. Martin, M. Martin, P. Muhlemann and C. Nef, *et al. Nucl. Phys. B* **184**, 1-12 (1981)
139. M. Bourquin *et al.* [Bristol-Geneva-Heidelberg-Lausanne-Rutherford], *Phys. Lett. B* **172**, 113 (1986)
140. A. N. Alev *et al.* [EXCHARM], *Phys. Atom. Nucl.* **56**, 1358-1366 (1993) JINR-D1-92-534.
141. D. Aston, N. Awaji, J. D'Amore, W. M. Dunwoodie, R. Endorf, K. Fujii, H. Hayashii, S. Iwata, W. B. Johnson and R. Kajikawa, *et al. Phys. Lett. B* **180**, 308 (1986) [erratum: *Phys. Lett. B* **183**, 434 (1987)]
142. M. S. Kholodenko [VES], *Phys. Atom. Nucl.* **83**, no.11, 1602-1606 (2020)
143. M. Ablikim *et al.* [BESIII], *Phys. Rev. D* **87**, no.3, 032008 (2013)
144. M. Ablikim *et al.* [BES], *Phys. Rev. D* **72**, 092002 (2005)
145. V. V. Anisovich and A. V. Sarantsev, *Eur. Phys. J. A* **16**, 229-258 (2003)
146. V. V. Vladimirov, V. K. Grigorev, I. A. Erofeev, O. N. Erofeeva, A. P. Zaitsev, Y. V. Katinov, V. I. Lisin, V. N. Luzin, V. N. Nozdrachev and V. V. Sokolovsky, *et al. Phys. Atom. Nucl.* **71**, 2129-2137 (2008)
147. A. V. Anisovich, C. A. Baker, C. J. Batty, D. V. Bugg, L. Montanet, V. A. Nikonov, A. V. Sarantsev, V. V. Sarantsev and B. S. Zou, *Phys. Lett. B* **542**, 8-18 (2002)
148. A. Etkin, K. J. Foley, R. W. Hackenburg, R. S. Longacre, W. A. Love, T. W. Morris, E. D. Platner, A. C. Saulys, S. J. Lindenbaum and C. Chan, *et al. Phys. Lett. B* **201**, 568-572 (1988)
149. J. Z. Bai *et al.* [BES], *Phys. Rev. Lett.* **76**, 3502-3505 (1996)
150. D. Aston, N. Awaji, T. Bienz, F. Bird, J. D'Amore, W. Dunwoodie, R. Endorf, K. Fujii, H. Hayashii and S. Iwata, *et al. Phys. Lett. B* **215**, 199-204 (1988)
151. R. M. Baltrusaitis *et al.* [MARK-III], *Phys. Rev. Lett.* **56**, 107 (1986)
152. C. Evangelista *et al.*, *Nucl. Phys. B* **154**, 381-393 (1979)
153. C. Caso, F. Conte, G. Tomasini, D. Cords, P. von Handel, H. Nagel, P. Schilling, G. Costa, L. Mandelli and S. Ratti, *et al. Lett. Nuovo Cim.* **3S1**, 707-713 (1970)

154. E. Klempt, K. V. Nikonov, A. V. Sarantsev and I. Denisenko, *Phys. Lett. B* **830**, 137171 (2022)
155. A. V. Anisovich *et al.* [Crystal Barrel], *Phys. Lett. B* **452**, 173-179 (1999)
156. A. V. Anisovich, C. A. Baker, C. J. Batty, D. V. Bugg, C. Hodd, J. Kisiel, V. A. Nikonov, A. V. Sarantsev, V. V. Sarantsev and I. Scott, *et al.* *Nucl. Phys. A* **651**, 253-276 (1999)
157. A. V. Anisovich, V. A. Nikonov, A. V. Sarantsev, V. V. Sarantsev, C. A. Baker, C. J. Batty, D. V. Bugg, A. Hasan, C. Hodd and B. S. Zou, *et al.* *Phys. Lett. B* **471**, 271-279 (1999)
158. A. V. Anisovich, V. A. Nikonov, A. V. Sarantsev, V. V. Sarantsev, C. A. Baker, C. J. Batty, D. V. Bugg, C. Hodd, B. S. Zou and J. Kisiel, *Phys. Lett. B* **468**, 309-313 (1999)
159. A. V. Anisovich, C. A. Baker, C. J. Batty, D. V. Bugg, A. Hasan, C. Hodd, B. S. Zou, J. Kisiel, V. A. Nikonov and A. V. Sarantsev, *et al.* *Nucl. Phys. A* **662**, 319-343 (2000)
160. A. V. Anisovich, C. A. Baker, C. J. Batty, D. V. Bugg, C. Hodd, H. C. Lu, V. A. Nikonov, A. V. Sarantsev, V. V. Sarantsev and B. S. Zou, *Phys. Lett. B* **491**, 47-58 (2000)
161. A. V. Anisovich *et al.* [Crystal Barrel], *Phys. Lett. B* **452**, 187-193 (1999)
162. A. V. Anisovich, C. A. Baker, C. J. Batty, D. V. Bugg, V. A. Nikonov, A. V. Sarantsev, V. V. Sarantsev and B. S. Zou, *Phys. Lett. B* **517**, 261-272 (2001)
163. A. V. Anisovich, C. A. Baker, C. J. Batty, D. V. Bugg, V. A. Nikonov, A. V. Sarantsev, V. V. Sarantsev and B. S. Zou, *Phys. Lett. B* **517**, 273-281 (2001)
164. D. V. Bugg, L. Y. Dong and B. S. Zou, *Phys. Lett. B* **458**, 511-516 (1999)
165. A. V. Anisovich, C. A. Baker, C. J. Batty, D. V. Bugg, V. A. Nikonov, A. V. Sarantsev, V. V. Sarantsev and B. S. Zou, *Phys. Lett. B* **496**, 145-153 (2000)
166. M. Ablikim *et al.* [BESIII], *Phys. Rev. D* **93**, no.11, 112011 (2016)
167. D. Bisello *et al.* [DM2], *Phys. Rev. D* **39**, 701 (1989)
168. D. Alde *et al.* [Serpukhov-Brussels-Los Alamos-Annecey(LAPP)], *Nucl. Phys. B* **269**, 485-508 (1986)
169. M. Atkinson *et al.* [Omega Photon], *Z. Phys. C* **29**, 333 (1985)
170. P. D. Barnes, G. Franklin, R. McCrady, F. Merrill, C. Meyer, B. Quinn, R. A. Schumacher, V. Zeps, N. Hamann and W. Eyrich, *et al.* *Phys. Rev. C* **62**, 055203 (2000)
171. D. V. Bugg, *Eur. Phys. J. C* **36**, 161-168 (2004)
172. M. Atkinson *et al.* [Omega Photon], *Z. Phys. C* **38**, 535 (1988)
173. M. Ablikim *et al.* [BESIII], *Phys. Lett. B* **813**, 136059 (2021)
174. A. Hasan and D. V. Bugg, *Phys. Lett. B* **334**, 215-219 (1994)
175. M. N. Oakden and M. R. Pennington, *Nucl. Phys. A* **574**, 731-754 (1994)
176. D. Cutts, M. L. Good, P. D. Grannis, D. Green, Y. Y. Lee, R. Pittman, J. Storer, A. C. Benvenuti, G. C. Fischer and D. D. Reeder, *Phys. Rev. D* **17**, 16 (1978)
177. D. Alde *et al.* [GAMS], *Nuovo Cim. A* **107**, 1867-1874 (1994)
178. A. Alde *et al.* [IHEP-IISN-LANL-LAPP-KEK], *Z. Phys. C* **54**, 553-558 (1992)
179. M. Ablikim *et al.* [(BESIII Collaboration)* and BESIII], *Phys. Rev. Lett.* **129**, no.4, 042001 (2022)